Using Quantified Motor Behavior Outcomes to Improve Deep Brain Stimulation in Parkinson's Disease

A DISSERTATION
SUBMITTED TO THE FACULTY OF
UNIVERSITY OF MINNESOTA
BY

Kenneth Howard Louie

IN PARTIAL FULLFILMENT OF THE REQUIREMENTS

FOR THE DEGREE OF DOCTOR OF PHILOSOPHY

Advisor: Théoden I. Netoff, PhD

Co-mentor: Scott E. Cooper, MD, PhD

June 2020

Acknowledgments

I would like to acknowledge the following individuals for their contribution and support:

Dr. Théoden I. Netoff: Thank you for your mentorship and support throughout my doctoral degree. Your positivity and dedication to details provided me with motivation to finish my degree and taught me how to think like a researcher. Truly, you help me become the research I have become, and put me in a position to pursue an academic career starting with a post-doctoral position in a fantastic lab.

Dr. Scott Cooper: Thank you for your mentorship and guidance in performing clinical research. The work I have done in your lab has opened research I didn't know was possible to conduct. Your approach to data analysis will always stick with me and have made me think more critically on what I am seeing in my data. We have had difficulties with the technical aspects of the projects I worked on, but I am glad we got past them together.

Past and present labmates in the Netoff, Cooper, and MacKinnon lab: Abbey Becker, Vivek Nagaraj, Jennifer Zick, Logan Grado, Zixi Zhao, Sadegh Faramarzi Ganj Abad, Chiahao Lu, Matthew Petrucci, Sommer Amundsen Huffmaster, Jae Chung, Maria Linn-Evans, and Rebekah Summers. Your support, collaboration, scientific feedback, and friendship were invaluable.

Research coordinators: Josh De Kam, Jacob Guizior, Emily Twedell, and Tessneem Abdallah. I couldn't perform any of my experiments without you.

All Parkinson's disease patients that participated in my study. I'm very grateful of the generosity you showed to take time out of your schedule and participate in my studies.

My girlfriend, Clairice Pearce. Your love, support and companionship helped me focus to finish this thesis, and pushed me to pursue a fantastic lab for my post-doc.

My family, particularly my parents Hans and Becky, my sisters Julianne and Tracy, and my grandpa Sam, for providing me with love, support, and enthusiasm in everything I have done. You taught me to be independent and hardworking.

Dedication

I dedicate this to my parents, Hans and Becky, for their love and support.

Table of Contents

List of Tables

List of Figures

Chapter 1 – Introduction

Parkinson's Disease

Background

Parkinson's disease (PD) is the second most common neurodegenerative disease[1,2], affecting approximately 680,000 individuals in the US alone.[3] First described by James Parkinson's in his 1817 essay "Shaking Palsy," the motor signs of bradykinesia, tremor, and rigidity are still used as indications of the disease. Axial symptoms, such as speech and gait, and non-motor signs, such as cognitive and sensory dysfunction[4], may be present as well.

On a cellular level, PD patients have high amounts of α-synuclein proteins that aggregate to form Lewy bodies.[5,6] As the amount of Lewy bodies increases, particularly in the substantia nigra pars compacta (SNc), cell death occurs.[5,7,8] This results in a decreased production of dopamine and alteration of the basal ganglia, a network of different nuclei that contribute to movement.[9]

The basal ganglia controls movement through three pathways, collectively known as basal-ganglia-thalamo-cortical loops[10,11] (Figure 1). These pathways work to promote (direct) and stop (indirect/hyperdirect) movement. The direct and indirect pathways work in conjunction to adjust how much movement to produce, while the hyperdirect pathway acts as an "emergency stop." To understand how these pathways influence movement, one can look at the activity of the thalamus. The thalamus provides excitatory input into the motor cortex, meaning an increase in activity would be pro-movement and a decrease in activity would be anti-movement. In the direct pathway, excitation of the striatum inhibits activity of the globus pallidus interna (GPi). An inhibitory projection from the GPi to the thalamus implies that the thalamus is more active, therefore promoting movement. In the

indirect pathway, the striatum inhibits the globus pallidus externa (GPe), which has inhibitory projections to the GPi and subthalamic nucleus (STN). Excitatory projections from the STN to the GPi implies the GPi is more active. The net result is an increase in activity of the GPi, which then inhibits the thalamus and is anti-movement. For completeness, the hyperdirect pathway excites the STN, which would inhibit the thalamus.

Dopamine was excluded in the explanation above but can be easily added in to understand how it affects the pathways. The substantia nigra pars compacta (SNc) produces the dopamine that is transported to the striatum. In the striatum there are two dopamine receptors, D_1 and D_2. The direct pathway is influenced by D_1-receptors, and activation of D_1-receptors increases activity of the inhibitory projections to the GPi. The indirect pathway is influenced by D_2-receptors. Unlike D_1-receptors, D_2-receptors act to decrease the activity of the inhibitory projection from the striatum to the GPe. Given what we know about the pathways, a release of dopamine causes a net increase in activity in the thalamus in healthy adults. With the loss of dopamine from the SNc, the tonic activity levels of the GPi and STN is increased, inhibiting movement.[12,13]

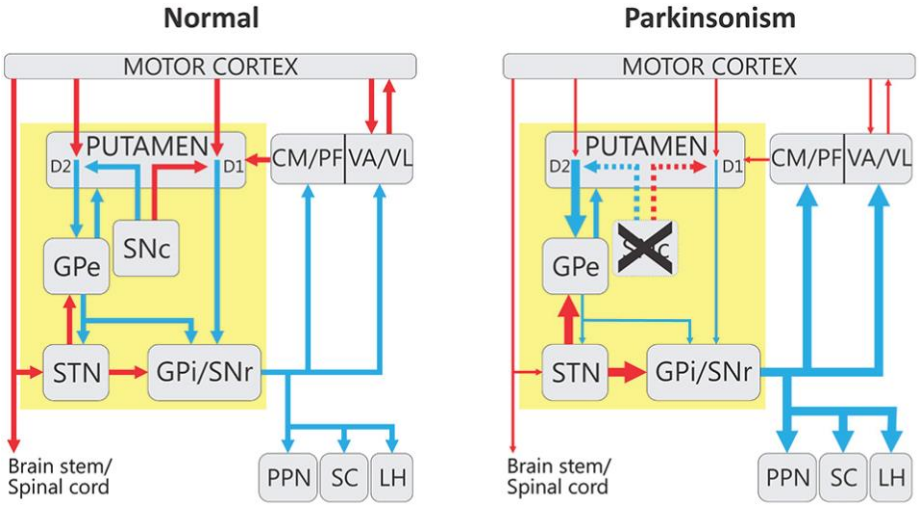

Figure 1. Basal ganglia circuit diagram for healthy and PD. (Galvan, Devergnas, Wichmann, 2015) Yellow box indicates the basal ganglia area of interconnected nuclei. Red and blue arrows indicates excitatory and inhibitory connection D1 and D2 indicate postsynaptic dopamine receptor type; GPe, globus pallidus externus; GPi, globus pallidus internus; SNc, substantia nigra pars compacta; SNr, substantia nigra pars reticulata; STN, subthalamic nucleus; and VA/VL, ventral anterior/ventral lateral of thalamus.

Clinical Assessments

Stages of neurodegeneration in human PD patients has been previously described by Braak et al.[5] "Braak" stages, as they were called, gained acceptance in the community[14,15] before critical evaluations have questioned validity of the stages.[16] The group received autopsy brains containing Lewy bodies and classified 6 different stages corresponding to degeneration of different areas. Degeneration of the SNc occurs at stage 3 and coincided with the first clinical diagnosis of PD in their brain samples. Characterization of the degeneration in living and pre-symptomatic patients has been done using positron emission tomography (PET).[17] However, only partial agreement between Braak staging and PET was concluded.[17]

Only recently has the characterization of different stages of PD been studied. Prior to these studies, clinical rating scales were developed. Currently, the two most frequently used scales are the modified Hoehn and Yahr (H&Y)[18] and Movement Disorders Society - Unified Parkinson's Disease Rating Scale (MDS-UPDRS).[19] The modified H&Y added half stages to the initial scale[20] and describes the location of the symptoms, severity, and presence of postural imbalance. MDS-UPDRS is also a modification of the original scale, the UPDRS[21], and is a more comprehensive clinical assessment. The MDS-UPDRS is split into 4 sections covering motor and non-motor complications of daily living, a motor performance examination, and motor complication. Motor performance is assessed solely by the clinician, where they score different motor signs including the cardinal signs of bradykinesia, tremor, and rigidity. In most cases, scores for H&Y and MDS-UPDRS are reported.

Treatment Options

There is no cure for Parkinson's disease, but a variety of treatment options such as medication[22], ablative surgery, and electrical stimulation[23] exist. Dopamine replacement therapy (DRT) is the standard treatment option where dopamine precursor levodopa, dopamine agonist, monoamine oxidase B inhibitors, or catechol-O-methyl-transferase inhibitors are taken by the patient[24]. While DRT has been very effective at treating the cardinal symptoms of PD, the effectiveness of the medication can wane and induced dyskinesias may appear.[25,26] A balance between symptom suppression and dyskinetic side effects requires adjustments of medication, but may not ultimately be achieved. When a balance cannot be achieved, the patient may elect to receive ablation surgery or deep brain stimulation (DBS).

Ablation surgery for PD involves lesioning of the thalamus, GPi, or STN. The effects are permanent, and any side effects are irreversible.[27–29] Although there is significant risk, there is an improvement of symptoms. Thalamotomy suppressed tremor in 80% of patients and increased activity levels.[27] Pallidotomy improved UPDRS scores by 35.5%, and patients reported marked or moderate improvement of their Parkinsonian symptoms.[30] Subthalamotomy reduced UPDRS sections II and III, and the improvement was maintained for up to 24 months.[29] A non-permanent therapy that achieves similar or better results is DBS.

Deep Brain Stimulation for Parkinson's Disease

A PD patient can expect to experience roughly a 20-50% improvement in their MDS-UPDRS scores following DBS[31–33], making it a highly effective therapy.[31,32,34–36]

DBS for PD involves the implantation of macro electrodes in the ventral intermediate nucleus of the thalamus (VIM), GPi, or STN. The leads of the implanted electrodes are connected to a pulse generator that delivers electrical stimulation continuously. After implantation, each patient undergoes "programming," where the optimal parameters are determined. These include the amplitude, frequency, pulse width, and electrode configuration. Amplitude and electrode configuration vary, but frequency is typically between 130-185 Hz, and pulse width between 60-120μs.[37] Improvements in motor signs are similar between STN and GPi stimulation[38–41], but GPi reduction of dyskinesia is thought to be greater.[39,42] The mechanism by which DBS, specifically at frequencies (≥130 Hz), works is debated.

Proposed Mechanism of Action

DBS has been theorized to inhibit[43,44] or excite neurons.[45] While evidence for both views exist, studies have sought to explain how both might occur.[46] This resulted in the current theory that DBS therapeutic efficacy comes from disrupting pathological oscillations.

Inhibition of neurons by DBS was first theorized as the method that produces the clinical effects seen in thalamotomies. Evidence for this theory has been shown in rats, non-human primates, and in human PD patients. In a rodent model of PD, stimulation of the STN at 130 Hz reduced spike rate of all recorded cell for 30-90 second after DBS was turned off. [43] Spike rate was also found to decrease in the STN of non-human primate models of PD[47,48], and found that the stimulation caused "burst-like" firing.[47] GPi spike rate was also found to be decreased with stimulation.[44] Dostrovsky et al. reported 22 of 23

cells recorded in the GPi, during DBS implantation surgery, had inhibited spontaneous activity following the stimulation. Parallel to the inhibition theory, groups have discovered increased activity following DBS.

Excitation of neurons have been examined through both excitatory and inhibitory synaptic connections in non-human primates. Hashimoto et al. reported increased activity in the GPi and GPe following STN stimulation.[45] Years later, Vitek et al. reported a decrease in firing rate in the STN and GPi when stimulating the GPe.[49] Both GPi and GPe have excitatory afferents from the STN, while the STN and GPi have inhibitory efferent from the GPe. Together, these studies have provided a strong argument that DBS functions through excitation of neurons.

But inhibition and excitation of neurons cannot occur simultaneously. Computational models have been developed to resolve this contradiction.[46] The models include cell bodies, axons, and a representation of a clinically available electrode. It was reported that stimulation from the electrode inhibits the cell body. However, action potentials were generated at the frequency of stimulation in the axon.[46] This data provided an explanation of what is seen experimentally, and led to a new hypothesis.

If neurons are inhibited and action potentials are generated in the axon at the frequency of stimulation, the therapeutic effect of DBS is caused by regular firing of nuclei in the network. This is known as the informational lesion hypothesis and explains why therapeutic efficacy depends on stimulation frequency.[50–52] At high frequencies of stimulation, there is little variation in activity in the stimulation nuclei and is thought to be lacking informational content. Containing little information implies that pathological activity is blocked. Thus, observing an improvement of Parkinson's motor signs.

Conversely, low frequency stimulation do not improve motor signs greatly and has been shown that the induced periodic activity is not sufficient to produce an informational lesion.[53]

Additional evidence for the informational lesion hypothesis has been provided through recordings of synchronous activity in extracellular space, otherwise known as local field potentials (LFP). Previously, it has been found that a frequency band, 13-30 Hz (beta), is naturally occurs to suppress spontaneous movement, indicating a stabilization of the current motor state.[54] In PD patients and non-human primate models, a consistent increase in beta band power is seen (Figure 2).[48,55–57] The elevated beta band power is attenuated when patients take levodopa[55,58] or receive stimulation to either the GPi or STN[59–62], with an improvement in motor symptoms proportional to the attenuation.[58,60,63] This indicates that DBS reduces the abnormally increased beta band power, blocking pathological information.

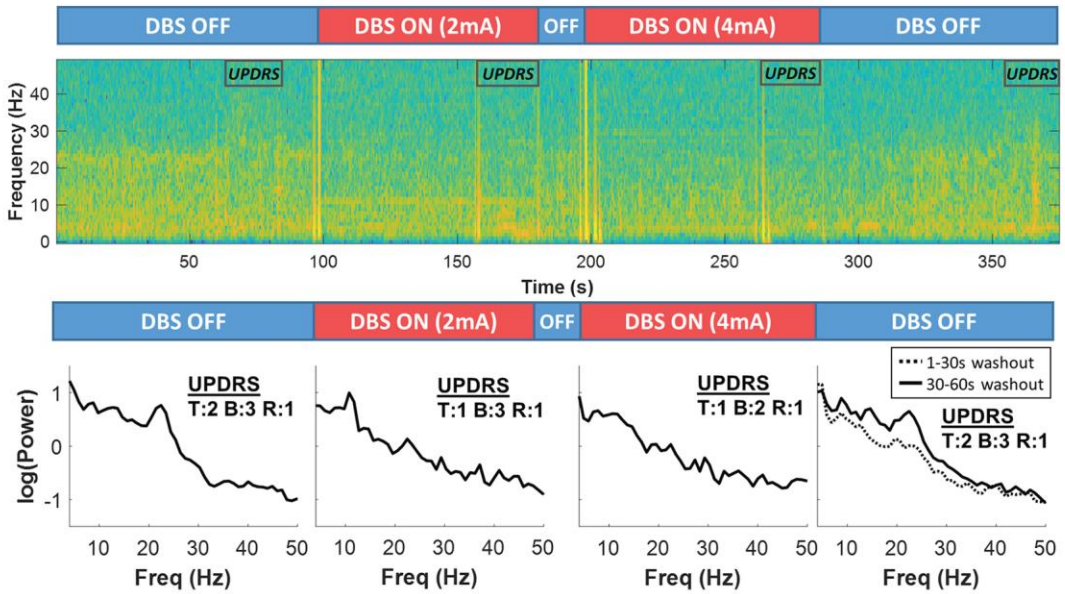

Figure 2. DBS effects on LFP in the GPi. Spectrogram of LFP recordings in the GPi over 6 minutes with DBS at different amplitudes. Beta band power (12-30 Hz) is decreased following DBS, and returns when the stimulation is turned off.

Time Course of Motor Signs Following DBS

When DBS is on, different time courses can be expected for different motor signs. Tremor and rigidity improve seconds after stimulation is on.[64,65] Bradykinesia is slower, taking approximately 2 minutes to improve.[65] Axial symptoms take the longest to improve, hours or days.[66] Interestingly, motor signs do not share a similar time course of return once DBS is turned off.

Temperli et al. was one of the first to examine the return of Parkinsonian motor signs after turning off stimulation[67], setting a guideline for many clinical experiments run today. The group found that there was a "sequential pattern of return," starting with tremor, followed by bradykinesia and rigidity, and finally axial symptoms. Tremor returns in minutes. Bradykinesia and rigidity can take between 30 minutes to 1 hour. Axial symptoms can take between 3-4 hours to return; although, axial UPDRS scores reach 90% of their off-stimulation levels after 2 hours. Taken together, between 1 and 2 hours of wash-out is commonly taken in clinical experiments. While these return time frames are used commonly, the study relied on UPDRS measurements which can be subject to bias.

A more detailed and objective characterization of return has been shown for bradykinesia. Cooper et al. attached angular velocity sensors onto the finger and thumb, and instructed the participant to tap the tips "as fast as possible" and "as wide as possible."[68] The power spectrum of the angular velocity was taken as the objective measure of bradykinesia. They found that the return of bradykinesia has two phases; a fast and slow phase. Each phase was examined and found that lateral stimulation of the STN is more attributed to the fast phase while medial stimulation of the STN contributes more to the

slow phase. This detailed characterization of bradykinesia has revealed to be more than return of the symptom and is likely to be seen with rigidity or axial symptoms.

Parameter Optimization

DBS efficacy is influenced by variety of elements. Before surgery, MRI brain images are captured and used to determine the tract of the electrode to the STN or GPi. However, image windowing can greatly affect the tract that is chosen to reach the nuclei as other anatomical landmarks are used to estimate boarders of the nuclei.[69] If errors are significant, the electrode may have suboptimal placement leading to poor efficacy or side effects. While the process has been improved with 3D models of the brain and the electrode[70–74], errors can still occur.

With intended target or suboptimal electrode placement, post-operative stimulation parameter tuning can greatly affect the outcome. The tuning is performed by the clinician and is a trial-and-error process that can take up to 50 hours.[75] Tuning involves going through each contact and increasing the amplitude in small increments (0.2-0.5 V) until benefits or side effects are observed[76]; this process is often called the monopolar review. If benefits without side effects are seen, the amplitude is further increased until side effects or the full amplitude range is explored. The contact with the lowest amplitude with clinical benefits and minimal side effects seen is selected. Cases where the monopolar review achieves unsatisfactory results, frequency, pulse width, bipolar electrode configurations, or a combination is attempted. For a more detailed discussion on DBS programming in the clinic, see Volkmann et al 2006.

Monopolar review, described above, was created as a guideline for programming electrodes with 4 contacts. Recent development of electrodes with more than 4 contacts, including a recent FDA approval of a segmented electrode design, have increased the difficulty of DBS programming where the monopolar review may not be feasible. Automated parameter selection are in development and rely on biophysical models of the patient.[77,78] In these algorithms, parameters are selected in a way to maximize the volume of tissue activated (VTA) of desired brain tissue while minimizing current spread to regions where side effects may occur.[79–81] There is a gap in literature on PD motor sign's response to these algorithms results. More work is needed for these algorithms to be adopted as the heterogeneity of brains could imply different areas may be more effective at treating symptoms.

Adaptive Stimulation

Clinicians are receiving more tools to help program DBS for PD. However, some PD patients will still experience difficulties. Stimulation induced side effects from stimulation can cause movement[82–84], speech[85], and mood changes.[86,87] Battery life can be depleted at a faster rate if therapeutic settings, such as amplitude, is high.[88,89] For these patients, turning on stimulation when needed or changing parameters if symptoms are worse may be beneficial. This stimulation strategy is commonly called adaptive DBS (aDBS).

aDBS has been tested in PD patients during externalization, a brief period where the leads of the electrodes are exposed, and recordings are possible. One of the first algorithm for aDBS turned stimulation on and off when a threshold for LFP beta band

power was passed.[90] When applying aDBS unilaterally in the STN, MDS-UPDRS score improved and stimulation time was reduced by 56% compared to conventional continuous DBS.[90] The results were replicated by applying the aDBS algorithm bilaterally in the STN, improving MDS-UPDRS scores by 43%.[91] In the unilateral and bilateral case, Parkinsonian medication was withdrawn overnight, but the effects of the aDBS algorithm may persist when paired with medication.[91] Interestingly, this aDBS algorithm has also shown to reduce side effects related to speech.[92] While this aDBS algorithm has shown good therapeutic effect immediately after implantation, it was unknown how well this algorithm would function months or years after implantation. Luckily, new pulse generators that can simultaneously stimulate, record, and be controlled externally have been approved.

The approval of more advanced pulse generators has led to aDBS algorithms applied to DBS patients that are internalized. Algorithms for these devices have used LFP power as the biomarker, as seen in previous studies[93–95], but other algorithms have used signals from external motor behavior measures.[96] The aDBS algorithms based on controlling LFP power have reduced tremor and bradykinesia when controlling beta[93,95], and reduced dyskinesia when controlling narrow gamma band (60-90 Hz).[94] These data show that aDBS can be therapeutic after the initial implantation, but perhaps the most interesting result has come from the aDBS algorithm using an external measure.

Cagnan et al. measured tremor in essential tremor patients in real-time to determine the appropriate time to deliver the stimulation pulses.[96] The group built a phase response curve and empirically selected the phase that maximally reduced tremor, reaching up to 87% tremor suppression. This study showed that external measures of motor behavior are viable signals to improve DBS efficacy and will be explored throughout this thesis.

Improving Deep Brain Stimulation in Parkinson's Disease Using Quantified Motor Behavior Outcomes

The past 18 years since the FDA's approval of DBS for PD has seen studies examine the mechanism of DBS, develop new tools, and new methods of stimulation. Taken together, the research has made DBS highly effect therapy for PD. However, current research to build tools or methods that further improve DBS efficacy need to be validated. Alternative approaches need to be studied. In this thesis I explore the use of quantified motor behavior outcomes to improve DBS efficacy in PD patients by developing patient-specific therapy approaches and characterizing stimulation's effect on gait. I first developed a parameter optimization approach using Bayesian optimization, real time measures of rigidity, and patient preference to automatically determine the best frequency to minimize rigidity (Chapter 2). Next, I developed a real time gait phase state dependent stimulation algorithm that selectively deliver short duration stimulation aimed to improve gait (Chapter 3). Lastly, I characterize gait's response to stimulation to better develop future therapies for gait (Chapter 4). The ideas presented here provide a framework for future developments of DBS therapy that includes, or exclusively uses, quantified motor behavior outcomes.

Chapter 2 – Semi-Automated Approaches to Optimize Deep Brain Stimulation Parameters in Parkinson's Disease

The work presented in this chapter has been submitted for review: Louie KH, Petrucci, MN, Grado, Logan, Linn-Evans ME, Lu C, Tuite PJ, Lamperski AG, MacKinnon CD, Netoff TI, and Cooper SE. Semi-Automated Approaches to Optimize Deep Brain Stimulation Parameters in Parkinson's Disease. *IEEE Transactions in Neural Systems and Rehabilitation Engineering.*

Introduction

A prolonged clinical optimization phase follows implantation of the neural stimulator in PD patients. During optimization, stimulation settings that provide the best therapeutic effects and minimal side-effects are determined. The current generation of DBS stimulators have multiple electrodes (4 to 8 contacts) and a wide range of stimulation amplitudes (voltage or current), frequencies, and pulse widths. There are millions of possible setting combinations. From a clinical perspective, the effective parameter space is much smaller. Many settings do not reach clinical effectiveness, have similar motor sign improvement, or are likely to induce side-effects and thus can be excluded from exploration.[76,97] Nonetheless, the determination of "optimal" stimulation settings requires the clinician to iteratively modify stimulation parameters to best alleviate the individual's motor signs. This can require 50 or more hours of tuning.[75] Following this process, improvements in Unified Parkinson's Disease Rating Scale (UPDRS) motor scores between 20-50% are often seen in individuals after the clinician has optimized parameters.[31–33] However, it is still uncertain whether the clinician has identified the best stimulation settings using this tuning approach given that a large proportion of the parameter space remains untested.

Selecting the optimum stimulation settings state is further limited by the subjectivity and poor resolution of the motor outcomes measures. The clinical standard to evaluate the efficacy of stimulation is through examination of motor signs such as rigidity, bradykinesia, tremor, and gait. The severity of these motor signs is assessed using the motor UPDRS, which assigns a score to each element of the exam with an ordinal value between 0-4. This method of assessment and ordinal scoring limits the accuracy of outcome

measurement, because it is subjective and limited in scope. Methods have been developed for the quantitative assessment of rigidity[98–101], bradykinesia[102–108], tremor[109], and gait[110–114], but these are rarely used to determine DBS settings.[115,116] We posit that determination of DBS settings can be substantially improved by using quantitative measures of motor signs obtained during standardized and controlled tasks. This approach increases the resolution of the outcome measure and removes potential bias.

Several methods to increase the efficiency of DBS programming have previously been proposed. These include algorithms to select stimulation parameters based on iterative clinical assessments of benefits and side effects.[76,97,117–119] Yet, the parameter space tested with these approaches is still limited, and it is unclear if the greatest efficacy for a given motor sign has been achieved. Others have attempted to use biophysical models to determine settings that create a presumed ideal electrical field within a region of interest.[77–81] These electrical fields are modeled to selectively activate the desired brain tissue and minimize current spread to structures that may cause side effects. However, these techniques rely on high-resolution imaging of the lead and brain. This approach also assumes that one particular anatomical stimulation target is the most efficacious. Yet, there is currently a lack of consensus on the best target region(s)[120] or neural elements for symptomatic improvement. Finally, the most effective site for one symptom may be different from the best site for another[121–123], and the best target may differ between patients.

Here we propose a semi-automated Bayesian optimization approach to tune stimulation parameters using quantitative real-time measures of motor function. We also modeled the patient preference to stimulation parameters using a probit Gaussian Process

based on pairwise comparisons. The Bayesian optimization approach used here is semi-automated as it depends on a clinician present to set parameters and to observe side effects. The potential advantage of this optimization approach is that it could provide a considerably more efficient method to converge on the most efficacious stimulation settings and could achieve more consistent DBS outcomes. Fast convergence could reduce costs by decreasing the duration of stimulation adjustment while also reducing the confounding effects of patient fatigue -- a significant factor when adjustments take hours to accomplish. Consistent outcomes potentially reduce bias from the clinician, reducing the variance in UPDRS motor score improvements. Optimization algorithms can also help optimally resample parameters of interest to improve accuracy and to assure that potentially good therapeutic settings have not been missed.

For the purposes of proof-of-principle, we chose to optimize stimulation frequency using real-time measures of forearm rigidity, obtained from a robotic manipulandum.[124] Rigidity was chosen as the motor outcome based on evidence that it quickly responds to DBS[67], reaching 75% of the total improvement seen in 5 minutes, thus providing a reasonable wash-in period to rapidly assess the effects of stimulation frequency. However, there has been recent studies that have suggested an faster detectable change within seconds.[101] Additionally, rigidity response to frequency may not be monotonic. Lower frequencies have shown to yield little to no effect. Conversely, stimulation at higher frequencies (>60 Hz) can produce a rapid and marked reduction in rigidity.[101,125]

There are two goals of this chapter, 1) develop a method for rapid and efficient semi-automated optimization of frequency to minimize rigidity, and 2) develop a method to determine an individual's preferred stimulation frequency. A comparison between

approaches will determine if the most efficacious settings differs from the patient's preference. While the study only looked at one motor sign and stimulation parameter, the benefits of optimization using the Bayesian approach is expected to be greater when generalized to more than one parameter.

Methods

Participant Demographics

Two individuals with PD (*Table I*) were tested, one with DBS targeting the internal segment of the globus pallidus and the other with DBS targeting the subthalamic nucleus. Both individuals showed significant improvements in motor sign severity (assessed using part III of the UPDRS) while on clinical stimulation settings compared to off stimulation (Participant 1: off DBS UPDRS III = 56, on DBS UPDRS III = 42; Participant 2: off DBS UPDRS III = 65, on DBS UPDRS III = 30). The protocol was approved by the local institutional review board and both individuals provided informed consent prior to participation. Testing was conducted in the off-medication state, with their last dose of Parkinson's medication taken at least 16 hours prior to their visit dates. Both participants were classified as having the akinetic-rigid subtype of PD based on the ratio between the participant's UPDRS tremor and bradykinesia scores.[126] Throughout testing, DBS amplitude, pulse width, and electrode contacts settings were fixed to their clinically optimized settings.

Table I Participant Demographics for Chapter 2

TABLE I
PARTICIPANT DEMOGRAPHICS

Participant ID	Age	Sex	Disease Duration (years)	Subtype	DBS Target	MDS-UPDRS III Rigidity (Side*)	Contacts	Amplitude	Pulse Width	Clinical Frequency	Optimized Frequency
Participant 1	53	M	16	AR	GPi	2 (L)	1-2-c+	4.5 V	60 µs	125 Hz	155 Hz
Participant 2	39	F	09	AR	STN	2 (R)	2-c+	2.7 V	60 µs	150 Hz	185 Hz

AR = akinetic-rigid
GPi = Globus Pallidus Interna, STN = Subthalamic Nucleus
* Side of the body tested
Contacts, amplitude, pulse width, and frequency settings are taken from the contralateral side of testing.

Rigidity Measurement

A custom-made robotic manipulandum (Entact, Toronto, CA) was used to quantify rigidity. The robotic manipulandum houses a handle attached to a servomotor allowing rotation about the supination-pronation axis of the forearm (Figure 3 A). A strain gauge is attached to the shaft of the handle and is used to measure resistive torque. Torque is obtained from the strain gauge data after it is passed through a 16-bit digitizer (National Instrument, Austin, TX) sampling at 1 kHz, followed by a digital low pass filter with a cutoff frequency of 20 Hz using a 2 pole Butterworth filter (Figure 3 B). To estimate the force the participant imposes on the handle, the torque is rectified and integrated with respect to time, thus obtaining a measure of angular impulse.[99] The slope (vs. time) of the angular impulse was taken as the Robotic Manipulandum Rigidity (RoMaR) value, as shown in Figure 3 C. This method of quantifying rigidity has been validated with PD patient's MDS-UPDRS Upper limb rigidity scores.[124]

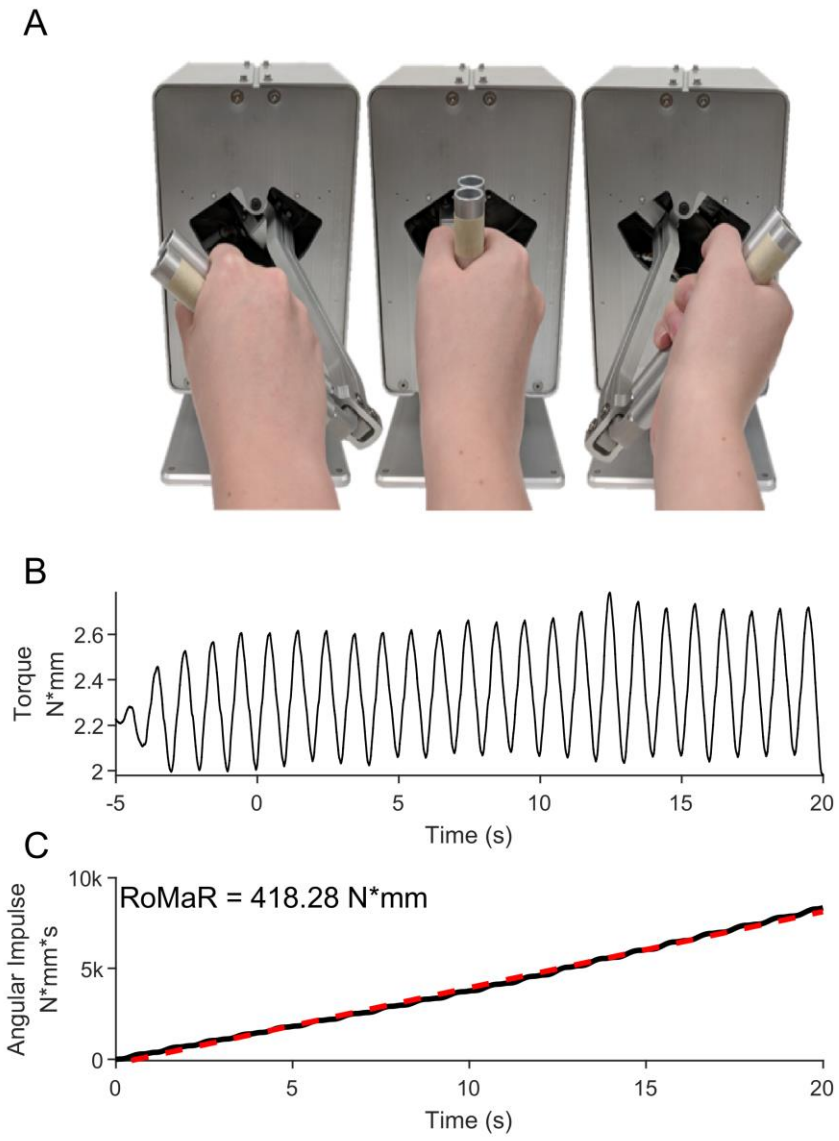

Figure 3. Rigidity Measurement. A) Robotic manipulandum. A participant is instructed to hold onto the handle as a motor moves it in a sinusoidal rhythm. Torque is measured through a strain gauge that is attached to the motor. B) Estimating rigidity from torque data. Torque data is low pass filtered with 20 Hz cutoff and measured over a 20 second trial after a five second warm-up. C) A patient's RoMaR value is calculated by measuring the slope of the impulse of the filtered torque signal (red line)

Optimization

Considerable effort is needed by our PD participants to obtain multiple RoMaR values. Participants were asked to come into lab off PD medication and stimulation turned off prior to the experiment. Furthermore, motor signs are not sufficiently alleviated during the experiment, making it difficult for the participant to reach the end of the experiment. Considering these issues, not all optimization algorithms are viable. An efficient and cost-effective algorithm is needed. In this study we used a semi-automated Bayesian optimization approach to sample the participant's specific rigidity-frequency relationship, as it has been shown to be efficient in terms of number of samples needed and useful when measurements are costly to obtain.[127–131]

Our objective function for the semi-automated Bayesian optimization algorithm only includes a quantitative measure of rigidity. However, motor sign improvement *and* side effects are considered during clinical optimization. To include side effects into Bayesian optimization, a quantitative measure is needed. Side effects are difficult to quantify accurately, and rather than incorporating a coarse measurement into the objective function, a comparison approach can be taken. In conjunction with Bayesian optimization, pairwise comparisons between subsequent stimulation frequency are used to create a probit Gaussian process preference model at the end of the experiment.

Bayesian Optimization

Bayesian optimization's (BayesOpt's) efficiency in sampling arises from incorporating prior beliefs about the input space with observations to build a model using Bayes' theorem,

$$P(M \mid E) \propto P(E \mid M)P(M).$$

This equation states that the *posterior* probability of the model M, given observations, E, is proportional to the likelihood of observing E given the model, multiplied by the *prior* probability of M. Once the model M has been built, BayesOpt operates on the model to direct sampling where it is beneficial to the goals of the optimization. Four steps are needed to run BayesOpt: 1) construction of a model from evidence, 2) estimate the mean and standard deviation at each frequency, 3) determine the utility of sampling at various frequencies, and 4) sample where utility is highest.

Various methods can be used to create a model from evidence, but a Gaussian processes (GP) is preferred because it meets many "simple and natural" conditions common in many optimization tasks[127].

$$f(x) \sim \mathcal{GP}\big(m(x), k(x, x')\big)$$

A GP is a generalization of the Gaussian probability distribution and can be thought as a *distribution over function*[132]. The GP is completely specified by its mean function, $m(x)$, and covariance function, $k(x, x')$, which measures the "similarity" between any two frequencies x and x'. The mean function is often set to 0, but was set to the mean RoMaR value after testing four frequencies in our study. For the covariance function, we used the Matérn kernel[133,134] as it offers flexibility between the smoothness of the input-output response and is among the most common kernels for GPs[131]:

$$k(x_i, x_j) = \frac{1}{2^{\nu-1}\Gamma(\nu)}\left(2\sqrt{\nu}\left\|x_i - x_j\right\|\right)^{\nu} H_{\nu}\left(2\sqrt{\nu}\left\|x_i - x_j\right\|\right)$$

where $\Gamma(\cdot)$ is the Gamma function, and H_{ν} is the Bessel function of order ν. Smoothness of the covariance function is balanced through the order parameter, ν, and the length-constant l. For this study, $\nu = 3/2$ as we expected to observe coarseness in the data but a

smooth trend, and estimated l using Matlab's hyperparameter optimization for each participant.

Now that we have built a model from our evidence, we can estimate the mean and standard deviation of RoMaR values at each frequency; this estimation is also called the *predictive* distribution. To calculate the *predictive* distribution, we incorporate all of our observations, $\mathcal{D}_{1:n} = \{x_i, f(x_i)\}$, with our GP model. Let us define a vector containing all values $\mathbf{f}_{1:n} = [f(x_1), \ldots, f(x_n)]$. An expression for the *predictive* distribution can be derived as,

$$P(f_{n+1} \mid \mathcal{D}_{1:n}, x_{n+1}) = \mathcal{N}(\mu_n(x_{n+1}, \sigma^2_{n+1}(x_{n+1}))$$

where

$$\mu_n(x_{n+1}) = k^T K^{-1} f_{1:n},$$

$$\sigma^2_n(x_{n+1}) = k(x_{n+1}, x_{n+1}) - k^T K^{-1} k.$$

We denote k as a vector of covariance $[k(x_{n+1}, x_1), \ldots, k(x_{n+1}, x_n)]$, and K as a matrix containing all covariance values where the i, j entry is the covariance $k(x_i, x_j)$.

We use the information contained in the *predictive* distribution to determine where to sample next. Using the mean and standard deviation, BayesOpt selects the frequency where the utility, $u(x)$, is greatest. In this study, utility was defined as the expected improvement to the model's estimated minimum at each frequency:

$$f(x) = \begin{cases} (\mu(x) - f(x^-))\Phi(Z) + \sigma(x)\phi(Z), if\ \sigma(x) > 0 \\ 0, if\ \sigma(x) = 0 \end{cases}$$

$$Z = \frac{\mu(x) - f(x^-)}{\sigma(x)}$$

where $x^- = argmin_{x_i \in x_{1:n}} f(x_i)$, $\Phi(\cdot)$ is the cumulative density function of a standard normal distribution, and $\phi(\cdot)$ is the probability density function of a standard normal

distribution. Sampling only where it is expected to improve the greatest can oversample an area of the input space and choose a local minimum as the optimized frequency. MATLAB provides a method to account for oversampling through an exploration ratio that balances exploration and sampling near the estimated minimum. We use the MATLAB's "bayesopt" function to calculate the utility at all frequencies using MATLABS's expected improvement function and set an exploration ratio of 0.5. MATLAB returns the frequency with the largest utility to sample:

$$x_{n+1} = argmax_{x_{n+1}} u(x_{n+1} \mid \mathcal{D}_{1:n}).$$

Sampling where the variance is greatest will provide new evidence and reduce the model uncertainty at that frequency, improving the GP model's estimation of the underlying rigidity response. However, the magnitude of the frequency could induce intolerable side effects in human participants. To safely test the frequency with the highest utility, a clinician was tasked with changing the frequency and monitor the participant for side effects. New evidence from sampling was used to update the GP model. For more information regarding experimental protocol see *Experimental Protocol*.

Probit Gaussian Process

An optimization algorithm depends on the metric used to measure the outcome. In previous sections, we have focused on optimizing rigidity, which ignores other symptom reductions and side effects caused by stimulation. The ultimate goal is not just to reduce rigidity, *but also to minimize side effects and improve overall quality of life*. Unfortunately, side effects and quality of life are difficult to measure, and to optimize for. Even if accurate rigidity and side effect measurements could be obtained during optimization, we would

have to choose a function that balances the value of rigidity and side effects into a single scalar value.

Instead, we can re-formulate the problem and attempt to optimize directly for the desired outcome: *patient preference.* Asking patients to provide ratings on a numerical scale is difficult for the patients, often inaccurate, and subject to cognitive biases.[135,136] However, humans excel at comparing options and expressing preference for one over the others.[137] In applications requiring human judgment, preferences are often more accurate than numerical ratings.[138,139]

In order to use binary preference data, we must reformulate the GP into a probit Gaussian process (pGP). In a pGP, instead of being able to directly sample the objective function, we must infer it from a set of binary observations. Our data is no longer a score at each setting, but is a set of ranked pairs $\mathcal{D} = \{a_i \succ b_i\}_{i=1}^{m}$, where $\succ$ indicates that a patient prefers setting a to b. We use $x_{1:m}$ to denote the m distinct comparisons in the training data, where a_i and b_i are two elements of $x_{1:m}$.

We model the value function $v(\cdot)$ for any setting as $v(\cdot) = f(\cdot) + \epsilon$, where $\epsilon \sim \mathcal{N}(0, \sigma^2)$ is normally distributed noise. The value function describes the value a patient derives from a given setting, with the noise term modeling uncertainty in the participant's preferences. Here, σ is set to 1, and is not learned. The challenge here is to learn f, where $f = \{f(x_i)\}_{i=1}^{n}$ is the value of the objective function at the training points.

We can now relate our binary observations back to the latent objective function using binomial-probit regression. An example of the probit procedure used to model a 1D function from a series of preferences is illustrated in Figure 4. Using this model, the probability that item a is preferred to b can be calculated as:

$$
\begin{aligned}
P\big(a_i \succ b_i \big| f(a_i), f(b_i)\big) \quad &= P\big(v(a_i) > v(b_i) \big| f(a_i), f(b_i)\big) \\
&= P(f(a_i) - f(b_i) > \epsilon_b - \epsilon_a) \\
&= \Phi\left(\frac{f(a_i) - f(b_i)}{\sqrt{2}\sigma}\right)
\end{aligned}
$$

where $\Phi(\cdot)$ is the cumulative distribution function of the standard normal distribution. The probability that a is preferred to b is proportional to the difference between $f(a)$ and $f(b)$, divided by the magnitude of the noise, σ[131].

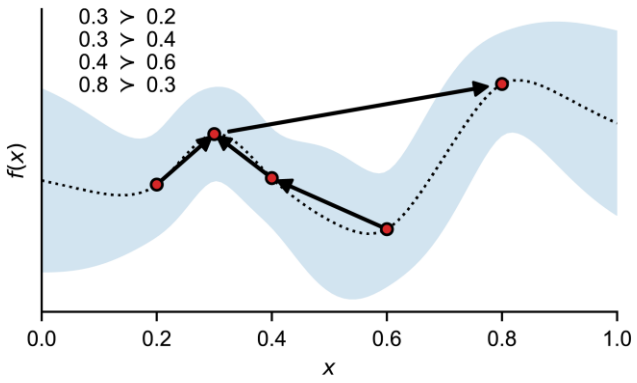

Figure 4. Probit example. Example of the probit model inferring a GP from a set of preference data. The preference data is shown in the top left, with corresponding arrows.

Now, we can estimate the posterior distribution of the latent objective function. Our goal is to find the distribution of the objective function which maximizes the posterior probability of our binary observations, known as the *maximum a posterior* (MAP) estimate. We use Newton-Raphson recursion to learn f_{MAP}.

$$f_{\text{MAP}} = argmax_f P(f|\mathcal{D}) \propto P(f) \prod_{i=1}^{n} P\big(a_i \succ b_i | f(a_i), f(b_i)\big)$$

Newton-Raphson recursion is subject becoming stuck in local minima, so multiple restarts with random initial conditions ($N = 25$) was performed.

After computing the model of the objective function, f_{MAP}, we can derive the predictive distribution of $P(f_{t+1}|f_{\text{MAP}}, \mathcal{D})$:

$$P(f_{t+1}|f_{\text{MAP}}, \mathcal{D}) \propto \mathcal{N}(kK^{-1}f_{MAP}, k(x_{t+1}, x_{t+1}) - k^T(K + C^{-1})^{-1}k),$$

where C is a matrix whose m, nth entry is given by

$$C_{m,n} = -\frac{\partial^2}{\partial f(x_m)\, \partial f(x_n)} \sum_{i=1}^{M} \log \Phi\,(Z_i)$$

and

$$Z_i = \frac{f(a_i) - f(b_i)}{\sqrt{2}\sigma}.$$

As before, k and K are the vector and matrix of covariances between inputs x.

Using the predictive distribution, we can then compute the utility and proceed with sampling as described in *Bayesian Optimization.*

Experimental Protocol

This study consisted of two visits. On the first visit, a brute-force approach was used to measure the RoMaR value at all frequencies, in pseudorandom order, between 10-185 Hz in increments of 5 Hz with two additional measures at the participant's clinical frequency. Frequencies that produced uncomfortable side effects were halted and all higher frequencies were not tested. On the second visit, RoMaR values was obtained at 30, 80, 90, and 140 Hz prior to BayesOpt guided programming. These frequencies were selected prior to the first participant and served a seed values to the GP model. They were selected to span the range of frequencies that would be comfortable for most PD patients with two samples near where the transition between ineffective and suppressive stimulation frequencies occurs in most patients. After testing at these seed frequencies, BayesOpt selected the next frequency to test for 8 iterations and incorporated frequency boundaries discovered during the first visit. One hour was allocated to testing, which included testing the 4 seed frequencies, data analysis and Bayesian optimization for setting selection, and the 8 tests, for a total of 12 rigidity measurements and 11 preference choices for each participant. The first rigidity measurement on each visit occurred after DBS has been turned off for one hour. For both visits, frequencies were programmed into the implantable pulse generator by a movement disorder specialist who could observe any notable side effects and terminate the stimulation if necessary (Figure 5).

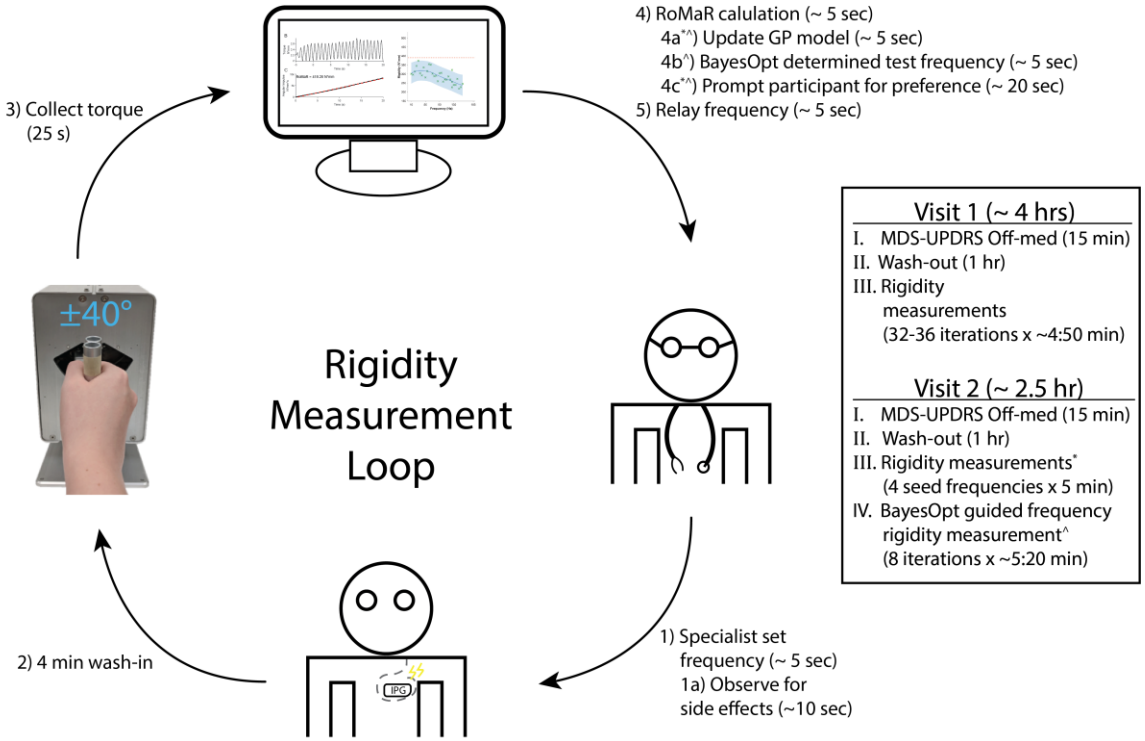

Figure 5. Loop schematic and experiment flow chart. Visit 1 and 2 both measure MDS-UPDRS and is followed by 1 hour of stimulation washout. After washout, rigidity is measured at all frequencies between 10-185 Hz during visit 1, and at 4 seed frequencies (30, 80, 90, and 140 Hz) during visit 2. Visit 2 then uses BayesOpt to guide frequency selection for 8 iterations. All rigidity measurements follows the loop diagram starting with the movement disorder specialist programming the frequency on the participant's implantable pulse generator.

Each rigidity measurement follows these steps: clinician sets stimulation frequency and monitors for side effects, four minutes of wash-in, custom software controlled 25 seconds of passive movement imposed by the manipulandum with a range of motion of ±40°, custom software calculation of the RoMaR value, and relay of the next frequency to the clinician. For visit 2 there are three additional steps: update of the GP model with the calculated RoMaR value, BayesOpt determined next frequency to test, and prompt the participant for frequency preference. Specifically, preference was asked with the following: “Which did you prefer, the current setting or the previous one, meaning the setting that felt best to you in terms of symptom reduction but also side effects?” In total, the time between each rigidity measurement takes approximately 5 minutes with the majority of that time dedicated to wash-in time.

Data Analysis

A GP was to fit to the patient data sampled using the brute-force and the BayesOpt methods, and a pGP was created at the conclusion of the BayesOpt experiment. Three metrics are derived from the GP models: 1) the optimal frequency, 2) Pearson's R correlation coefficient between the GP curves estimated from the two data sets, and 3) the frequency range considered indistinguishable from the minimum. The optimal frequency for rigidity suppression was estimated where the GP model's mean was at a minimum. The frequency range was estimated as all frequencies whose rigidity scores fell within one standard deviation of the value at the minimum. We then compared the optimal frequency found between BayesOpt and the brute-force approach. We also compared the Pearson's R correlation coefficient between the two curves and frequency range estimated using the BayesOpt and brute-force sampling methods. We also simulated two other sampling methods from the brute-force data and estimated the accuracy of the different

approaches as we gathered data and compared the estimated curves to the final brute-force curve. One simulated approach was to sample at a fixed interval of 5 Hz, between 10 Hz and the maximum frequency each participant could tolerate. The second simulated approach randomly selected frequencies, with repeats allowed. Lastly, we analyzed the peak of the participant's stimulation frequency preference model to the optimal frequency of the BayesOpt GP model.

Results

The objective of the study was to test how a semi-automated BayesOpt algorithm's setting selection may identify the optimal DBS stimulation frequency for maximal rigidity reduction efficiently and reliably as compared to a brute-force methods as well as to estimate a participant's preferred stimulation frequency. Two participants had two separate visits for optimization. In the first visit, the stimulation frequency was systematically tested at 30 frequencies for Participant 1 and 34 frequencies for Participant 2. For Participant 1, only stimulation frequencies at or below 155 Hz were tolerable. In total, visit 1 (brute-force method) testing took ~4 hours. In the second visit (BayesOpt approach), the rigidity response curve to stimulation frequencies tested were selected during the study using the BayesOpt algorithm. During the BayesOpt experiment, we also asked patients to report which stimulation setting they preferred, the current stimulation frequency or the previous frequency tested, to estimate their preference for stimulation frequency. The pairwise comparisons were then quantified to provide a value of each setting using a pGP. Visit 2 testing (BayesOpt) took ~2.5 hours. Here we report four results: (1) how rigidity is dependent on stimulation frequency, (2) a comparison of rigidity's dependency on frequency fit with GP models from the brute-force and the BayesOpt sampling, (3)

evaluation of the efficiency in estimating the rigidity-frequency curve using BayesOpt, and (4) the participant's preference for stimulation frequency, as estimated using the pGP.

In both participants we observed that stimulation frequency greater than 80 Hz was more effective at reducing rigidity than low frequency stimulation (Figure 6, Brute-force). Interestingly, 10 Hz in both participants reduced rigidity greater than 20-50 Hz stimulation. Rigidity did not follow a steady decrease after 50 Hz for Participant 2, where rigidity was higher between 130-155 Hz than frequencies around it. Participant 1 did show a steady decrease after 50 Hz, where their rigidity suppression was proportional to the stimulation frequency.

Rigidity was minimized at the highest frequency tolerated, or tested, at 155 Hz for Participant 1 and 185 Hz for Participant 2 during their brute-force visit (Figure 6, Brute-force Red dot). Their estimated optimal frequency from their BayesOpt visit matched the brute-force visit, and the GP models had comparable accuracy. The frequency range in the brute-force model for Participant 1 is 38 Hz wide and 96 Hz wide for Participant 2. Additionally, we measured the Pearson's R score between a participant's brute-force and BayesOpt sampled rigidity response curve. The two methods showed strong agreement with R scores of 0.98 and 0.94 for Participants 1 and 2 respectively. Participants 1's BayesOpt rigidity response curve mirrored the brute-force method with fewer evaluations, despite the Participant exhibiting higher RoMaR values on their second visit (Figure 6, top row). The range over which there was a reduction in rigidity was smaller in Participant's 2 BayesOpt visit, but the decrease in rigidity above 50 Hz was preserved (Figure 6, bottom row).

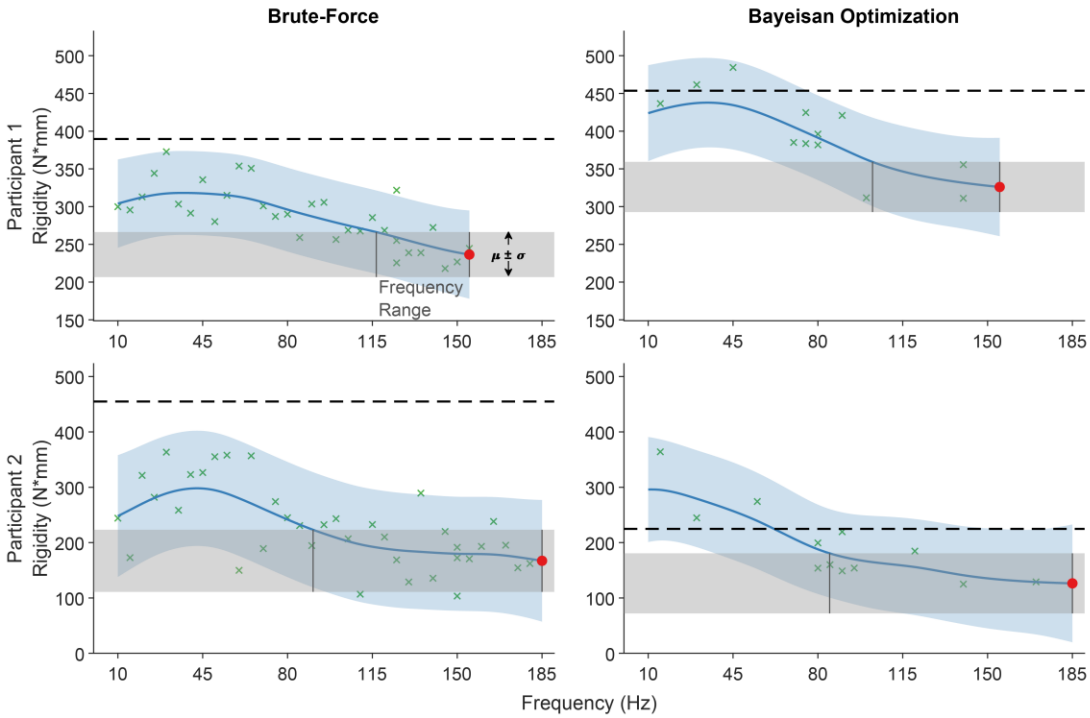

Figure 6. GP fits for Brute-Force and Bayesian Optimization visits. Two PD participants (column) have had their rigidity response curve measured using two different sampling methods (row). Brute-force method tested all frequencies spaced by 5 Hz from 10-185 Hz, and sampled in pseudorandom order, top row. Bayesian optimization guided frequency testing for rigidity, bottom row. *Black dashed lines* indicate the participant's RoMaR value after 1 hour off stimulation. *Red dot* indicates the estimated frequency that minimizes rigidity. *Shaded gray* region indicates RoMaR values within μ ± σ of the optimal frequency and the frequency range is defined as all frequencies whose estimated RoMaR values fall within this range and is indicated by the two thin vertical lines.

Efficiency of the BayesOpt algorithm was evaluated through comparison between two different sampling methods: equal spacing and random sampling of the frequency space. We then compared the curves from the GP fit to the sampled data to the final brute-force curve using the Pearson's R coefficient. We also compared the frequency range around the minimum across the different sampling methods.

Using only the initial sample frequencies (30, 80, 90, and 140 Hz), a GP fit model results in a curve very similar to the final brute-force measured curve with an R score of 0.99 for Participant 1 and 0.97 for Participant 2 (Figure 7, top: blue circles). However, these initial frequencies were selected to be good starting points, but we do not expect the quality of the curve based on the 4 points to be very robust. Upon further sampling the participants curve using BayesOpt, the R scores decrease before returning to higher scores again. Equal spaced sampling achieves a reliable fit to the final curve around 15 samples, with some significant fluctuations in the model until then, while BayesOpt has similar performance much more reliably (Figure 7, top: purple squares). The performance of random sampling, which was simulated 50 times, was significantly worse than evenly spaced sampling or BayesOpt (Figure 7, top: orange triangle).

The frequency range over which the rigidity was considered indistinguishable from the minimum was also compared across the different sampling methods. In this metric, the range decreased most rapidly using the random sampling and BayesOpt method, while even sampling had the worst performance (Figure 7, bottom: blue circles). In both patients, the range of the minimum rigidity was narrowed to its final range by 10 samples.

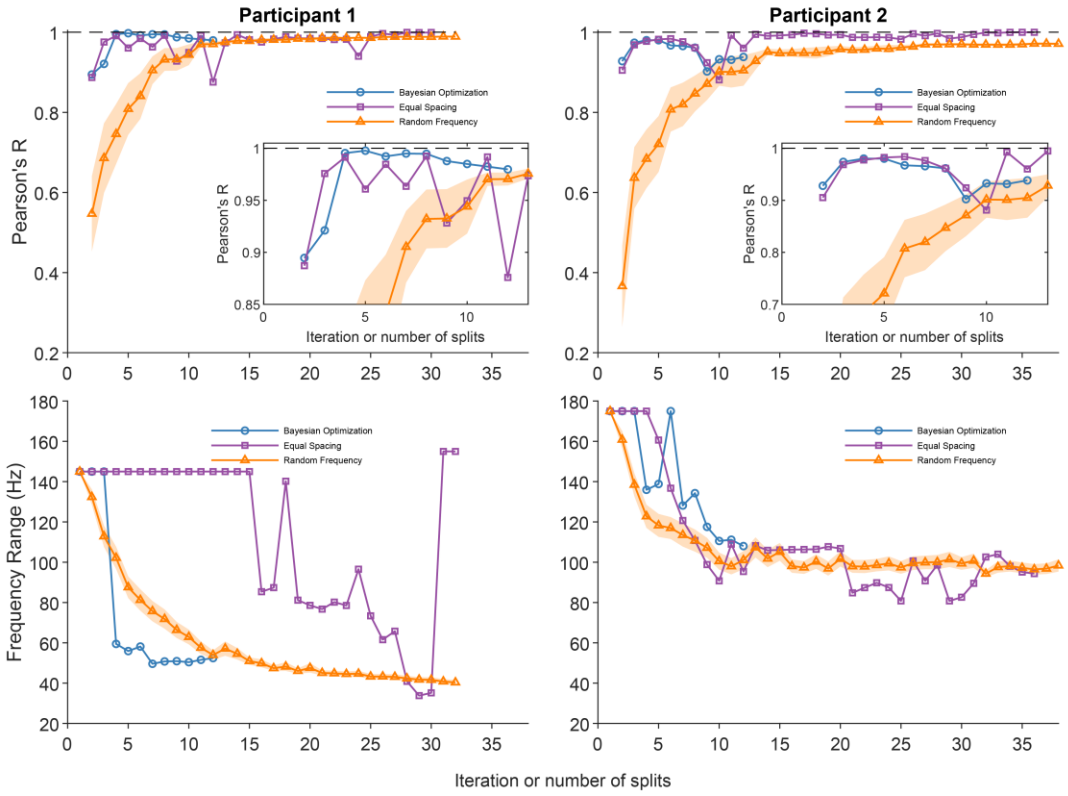

Figure 7. Bayesian Optimization Efficiency. Pearson's R correlation coefficient (top) and frequency range (bottom) after each iteration, or sample, of Bayesian optimization (*blue circles*) and two post-hoc frequency selection methods. The first post-hoc frequency selection method sampled every 5 Hz (*purple squares*). The second method randomly selected frequencies (*orange triangles*), and the shaded light orange region indicates the standard error of 50 simulations at each iteration. Pearson's R is calculated between the brute-force GP model and each selection method. The frequency range measured the distance between the optimal frequency and the lowest frequency that is contained within the optimal frequency's mean and standard deviation. A zoomed in window of Pearson's R correlation values allows for better comparison between sampling strategies (*inset plots*).

While testing different stimulation frequencies during Bayesian optimization, we asked patients to evaluate which setting they preferred: the current or previous setting. Based on the pairwise comparisons, the value of settings as a function of frequency was estimated using a probit Gaussian process. Figure 8 shows the GP fit to the rigidity-frequency and pGP fit for preference-frequency for both participants. Both participants *did not* prefer frequencies that provided the minimum rigidity scores at the top of the stimulation frequency range, as one might expect. Instead, they preferred frequencies between 70-110 Hz that were just high enough to have close to the maximal suppression of rigidity. Participant 1 strongest preference is at 70 Hz, and Participant 2 at 89 Hz.

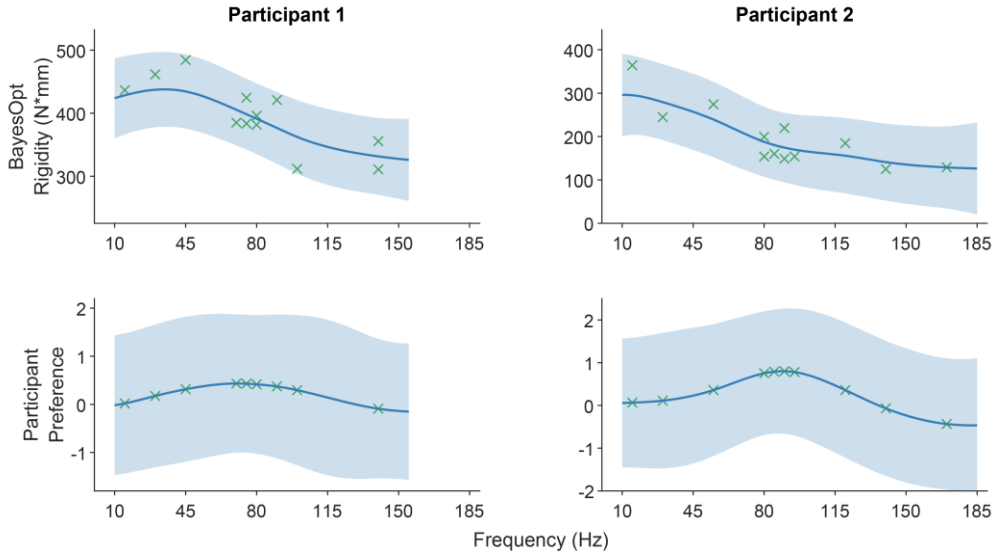

Figure 8. Probit Gaussian process fits. Rigidity response to frequency model after BayesOpt compared to preference model. The BayesOpt model was created after 12 iterations of the algorithm. The participants were asked which setting they preferred (the current or previous frequency setting). This was used to obtain their preference model.

Discussion

Here I have demonstrated the feasibility of a semi-automated Bayesian optimization approach to model a Parkinson's disease participant's rigidity response by rapidly and efficiently exploring a single stimulation parameter (frequency). Additionally, I explored the difference between an individual's preference and response model. By using Bayesian optimization, the optimal frequency for maximum reduced rigidity was determined from fewer sampled frequencies than those using the brute-force estimation method. Bayesian optimization also reduced the frequency range quickly, improving the confidence that the optimal frequency was found. When compared to random sampling, equally spaced sampling, and BayesOpt methods, BayesOpt was able to more efficiently and reliably estimate the rigidity's sensitivity to frequency and narrow down the frequency range where the minimum rigidity is observed. Considering balancing the accuracy of the curve fit and narrowing the range of the frequency range around the minimum rigidity, this suggests that BayesOpt is the most successful sampling algorithm. When measuring patient preferences between different frequency settings, I found that their preferred stimulation frequency is not at the frequency where rigidity is most suppressed, but at the minimum frequency at which rigidity significantly suppressed.

The pGP models constructed from the patients' preference revealed that both participants preferred stimulation frequencies that differed from the frequency that maximally reduced rigidity. The difference may be explained by the limitation of the RoMaR value to capture side effects of the stimulation. Side effects of DBS include motor and non-motor effects. Some motor side effects, such as dyskinesia, are easily detectable by an examiner, but more subtle or non-motor side effects like mood changes[86,87] may be

apparent only to the patient. Impairment of verbal fluency, induced at higher stimulation frequencies[85], is another subtle symptom. Our probit Gaussian process findings indicated a stronger preference to frequencies lower than what maximally suppresses rigidity. Given the prompt that is asked to the patient, the preference they select may indicate a balance effects of multiple symptoms and side effects. How patients weigh the significance and severity of multiple factors might differ among individuals and is an open question for future research.

We tested participants with a predominantly akinetic-rigid subtype of PD because we expected that rigidity in these individuals would have a strong dependence on stimulation parameters. This was reflected in the high Pearson's R score between the brute-force and the BayesOpt frequency response curves. For these reasons, our findings may only be applicable to people with a similar phenotype. However, the efficacy of DBS on other motor signs, such as tremor and bradykinesia, is also dependent upon stimulation frequency.[140,141] Accordingly, this semi-automated approach could be applied to optimize other motor signs that can be readily be quantified in real-time.

The data set is limited, and the technique may not extend to other participants with varying disease history. Participants in this study were classified as the akinetic-rigid subtype of PD and had disease durations of 9 and 16 years. Patients who are tremor dominant may not have rigidity that responds strongly to frequency. Additionally, patients that are in the early stages of PD may not present with RoMaR values greater than healthy older adults. However, the average disease duration prior to receiving DBS therapy is 13 years.[89] This duration is greater than Participant's 2 disease duration. Also, while tremor dominant subtype patients may not benefit from this approach, our findings indicate that

akinetic-rigid subtypes can benefit. Furthermore, our results also indicate that the BayesOpt approach can be effective regardless of stimulation target. Participant 1 had stimulation target in the internal segment of the globus pallidus, and Participant 2 had stimulation in the subthalamic nucleus. Both subjects showed a similar rigidity response to changes in frequency, which is in broad agreement with previous studies showing that the motor benefits of DBS are similar between the two targets.[33,39–41,142,143] Given the results of the study, we expect similar outcomes in a larger group of akinetic-rigid PD subtypes for rigidity.

A potential confound in this study was the duration of time between visits. In Participants 1 and 2 the time between visits were 4.5 and 9 months respectively. These time periods are sufficiently long that expression of rigidity may have changed between tests. In a 5-year longitudinal study, Holden et al. found that clinical motor scores increased 2.4 points per year.[144] For Participant 1, an increase in the UPDRS III right arm rigidity scores increased by one ordinal point from visit 1 to 2, and this is reflected in the higher RoMaR values seen during visit 2. Participant 2, however, had no change in clinical rigidity score, and but their RoMaR values were lower during visit 2. This may reflect day-to-day fluctuations in motor signs and differences in medication wash-out between visits which are not captured by the clinical rating scoring system. Nonetheless, despite changes in the mean in RoMaR values, the shape of the response curve was consistent for both the brute-force and the BayesOpt measured curves.

While this study focused on optimizing RoMaR values alone, total energy delivered (TEED) may also be considered[145] when optimizing stimulation parameters. However, it has also been observed that TEED may not play as critical of a role as the frequency when

tuning stimulation parameters.[146] If one desires to add TEED to the optimization, TEED may be scaled and then added to the RoMaR value for a total cost. Alternatively, stimulation amplitude can be adjusted to compensate for changes in frequency to keep TEED the same across the study. In this study, we neither accounted for nor compensated for changes in TEED in the optimization. In a study by Rizzone et al. showed that lower frequencies required a larger stimulation amplitude than higher frequencies to reach clinical effectiveness.[117] Therefore, in our study, the TEED may have been below therapeutic levels with stimulation at low frequencies. Keeping TEED constant may be beneficial when optimizing for one stimulation parameter but may introduce difficult trade-off considerations when optimizing over several parameters. For example, shortening the battery life to obtain the greatest reduction in motor signs.

Both approaches in this study are semi-automated to show proof-of-principal, but the goal is to create a fully automated closed-loop algorithm that incorporates additional motor signs and stimulation parameters. To achieve a fully automated closed-loop BayesOpt algorithm, objective measures of side effects, a single metric of the tested parameter's efficacy, and external software access to the patient's implantable pulse generator are needed. Currently, no methods exist for automated side effect detection. A single metric of the parameter's efficacy can be simple. For example, one could normalize all measures to the patient with their off-stimulation baseline, and simply sum the measures to create a single metric. More complex combinations of metrics are possible, such as adding weights to different motor sign measures. Direct programming of an implantable pulse generator from a computer is only available with Medtronic series of brain

stimulators, currently limiting an automated approach, but in the future we expect more stimulators will be programmable.

A fully automated closed-loop algorithm may also be built off of patient preference data, rather than quantified metrics of motor scores. A patient could test settings and evaluate their preferences and BayesOpt can be used to suggest new settings to test. The advantage of this approach is that patient preference may account for side effects that may be difficult to measure quantitatively and include in a cost function for optimization.

As implantable stimulators get more complicated and clinicians are provided with more flexibility, the opportunity to create better patient specific settings will be offset by the time it takes to find those optimal parameters and the complexity of the search. Efficient tuning will be necessary, especially when motor signs with long wash-in and wash-out times are evaluated. For the motor signs of bradykinesia and tremor, effects of stimulation can be seen within a couple of minutes.[67] Since our protocol allows for 4 minutes of wash-in time, both motor signs can be evaluated after this period with additional time (1 minute) for each measurement. If measurements of gait are added, *1 hour* of wash-in time is needed before evaluation.[67] Approximately 30 steps are needed to measure gait, collected over 2 minutes.[147] Using an approach like BayesOpt enables testing stimulation setting effects on such motor signs that otherwise would not be possible with other approaches given the constraints of a clinical visit and the endurance of a patient.

Conclusion

In summary, this study provides proof-of-principle of setting selection using a semi-automated BayesOpts for tuning frequency to minimize rigidity scores and pGP for

evaluating patient preferences. BayesOpts provides a rigorous approach to efficiently and accurately determining the optimal frequency to reduce rigidity, and pGP can assign a quantitative value to outcomes that are difficult to quantify in an objective optimization of stimulation parameters. BayesOpt efficiently finds optimal stimulation parameters and can be expanded to include additional motor signs and stimulation parameters. This is particularly important given the recent introduction of multi-segmented stimulation leads, and this approach may lead to improved patient outcomes.

Chapter 3 – Gait Phase Triggered Deep Brain Stimulation in Parkinson's Disease

The work presented in this chapter is being finalized for submission: Louie KH, Lu C, Netoff TI, and Cooper SE. Gait Phase Triggered Deep Brain Stimulation in Parkinson's Disease. *In Preparation for: IEEE Transaction on Neural Systems and Rehabilitation Engineering.*

Introduction

Gait disorder is one of the most disabling symptoms of Parkinson's disease (PD) and one of the most refractory to treatment. Following deep brain stimulation (DBS) therapy of the subthalamic nucleus (STN) or globus pallidus internus (GPi), spatial and temporal gait parameters can improve.[148–157] Yet gait is not considered to be adequately treated.[158]

Dissatisfaction with STN and GPi stimulation to treat PD gait led to interest in stimulation of the pedunculopontine nucleus (PPN).[159–163] However, results of clinical trials targeting PPN have been mixed.[164] Potential explanations of the varied results have included unoptimized programming and suboptimally located leads.[164] Other approaches to improve gait outcomes of stimulation are needed.

Two alternatives to conventional continuous DBS have been proposed to improve results: adaptive DBS (aDBS) and responsive DBS (rDBS). aDBS regularly changes stimulation parameter(s) whereas rDBS changes the timings of stimulation. Common between approaches is the necessity of a control signal. For aDBS, the predominant control signal has been power in the beta band (13-30 Hz) extracted from recorded local field potential. Control signals for rDBS will depend on what the stimulation is responding to. Only one study of rDBS has been reported and the control signal used was a motor behavior measure of tremor.[96] Initial studies have shown beta band aDBS and motor behavior rDBS can achieve similar efficacy and increased efficiency as compared to conventional continuous DBS.[90,91,93,94,165] Application of aDBS and rDBS primarily focuses on the motor signs of bradykinesia and tremor. Only one study has examined the effects on gait.[166] Although the study showed improved gait, it was in only one patient. More research into

aDBS or rDBS algorithms to treat gait is needed. Recent studies have indicated a relationship between a patient's beta power and gait cycle that could be used as a control signal.

Activity modulation with phases of gait has been shown with local field potential recordings in human PD patients. Oscillations in the theta-alpha (6-11Hz)[167] and beta[168,169] band correlate with increases in power during early swing and stance phase, with slight decreases or no change in band power outside of these phases. However, conventional continuous DBS causes a sustained decrease in beta-band power.[59,170,171] Suppressed beta-band power throughout the gait cycle may suppress functionally useful modulation of beta. Thus, rDBS timed to gait events might allow or enhance useful beta modulation of the LFP, which could then improve gait.

In this chapter, I develop an rDBS system to deliver short duration pulse trains at specific gait phases in real-time. To assess the accuracy of stimulation delivery, gait phases were aligned with stimulation artifacts collected from a surface EMG electrode on the neck. I also analyzed spatial and temporal gait metrics to determine the efficacy of the rDBS algorithm. This is the first study to explore this type of responsive gait phase stimulation to treat gait in PD patients.

Methods

Participants

Twelve PD individuals with bilateral DBS leads (9 STN and 3 GPi) and Medtronic SC, PC, or RC implantable neural stimulators (INSs) (Medtronic Inc., Minneapolis, MN) participated in the study (*Table II*). Participants were tested after overnight withdrawal of

PD medication prior to the study. All participants gave informed consent according to a University of Minnesota Institutional Review Board approved protocol.

Table II Participant Demographics for Chapter 3

TABLE II
PARTICIPANT DEMOGRAPHICS

Participant	1	2	3	4	5	6	7	8	9	10	11	12
Age	65	64	50	52	72	65	83	58	58	63	54	39
Sex	M	M	M	F	M	M	M	F	M	M	M	F
Disease Duration	26	13	12	12	6	10	10	24	14	6	5	9
Gait Speed Overground (m/s)	0.65	0.45	0.96	0.65	0.80	1.10	1.08	1.47	1.17	1.15	1.14	1.10
Gait Speed Treadmill (m/s)	0.42	0.23	0.96	0.49	0.80	1.10	1.08	1.47	1.17	1.15	1.14	1.10
Stimulation Target	STN	STN	STN	STN	STN	GPi	STN	STN	GPi	STN	GPi	STN
MDS-UPDRS III												
Total	37	70	80	68	35	36	37	31	30	12	12	56
Clinical Settings												
Contacts												
Left	c+1-2-	1+0-	3+1-	c+1-	c+2-	1+2-	c+3-	3+1-2-	c+2-	c+1-	c+2-	c+2-
Right	c+5-	c+0-	c+10-	1+0-	c+9-	3+2-	c+2-	c+6-7-	c+2-	3+1-	c+1-	c+10-
Amplitude												
Left	3.2 V	2.8 V	4.1 V	0.5 V	1.4 mA	5.2 V	3.0 V	3.2 V	3.6 V	2.9 V	3.4 V	2.9 V
Right	3.2 V	2.6 V	3.0 V	1.5 V	2.0 mA	5.0 V	3.8 V	3.0 V	3.5 V	3.1 V	2.8 V	2.9 V
Frequency (Hz)	160	130	180	180	130	130	130	130	180	130	130	150
Pulse Width (μs)												
Left	60	60	90	60	60	60	60	70	60	60	60	60
Right	60	90	90	60	90	60	60	70	60	60	60	60
Experimental Settings												
Contacts												
Left	c+1-2-	c+1-	c+1-	c+1-	c+2-	c+2-	c+3-	3+1-2-	c+2-	c+1-	c+2-	c+2-
Right	c+5-	c+1-	c+10-	c+1-	c+9-	c+2-	c+2-	c+6-7-	c+2-	3+1-	c+1-	c+10-
Amplitude												
Left	3.0 mA	2.0 mA	2.5 mA	0.4 mA	1.4 mA	3.5 mA	2.5 mA	3.0 mA	3.5 mA	2.5 mA	3.0 mA	2.7 mA
Right	3.0 mA	2.5 mA	3.0 mA	1.0 mA	2.0 mA	2.5 mA	3.5 mA	3.0 mA	3.5 mA	1.6 mA	2.5 mA	2.5 mA

GPi = Globus Pallidus Interna, STN = Subthalamic Nucleus

Experimental Protocol

Gait was first assessed by having participants walk 20 ft in a hallway 12 times to determine individual overground walking speed while on DBS. Afterward, DBS was turned off and wireless sensors were placed on the participant for gait phase detection used to trigger stimulation. An additional wireless sensor was placed for stimulation delivery timing analysis. The sensors (Trigno, Delsys Inc., Natick, MA) included force sensitive resistors (FSR) on the soles of the feet, accelerometers on the shanks, and surface EMG sensors on the neck, to detect stimulation artifact. In a few cases, bipolar clinical settings were approximated by monopolar settings for better artifact detection. Clinical voltage amplitudes were converted to equivalent current amplitudes, and experimental stimulation was delivered in constant current mode. This allowed for possible short-term changes in impedance as stimulation was turned on and off. Once sensors were placed and after a minimum of 1-hour DBS washout, gait metrics were measured on the treadmill at three different walking speeds: 100, 85, and 75% of their baseline overground walking speed. For two participants, additional trials at 65% and 50% were done because 75% was too difficult. The fastest speed that the participant could tolerate was used for further testing.

Then, participants performed one-minute trials of walking on the instrumented treadmill (C-Mill, Motek, Netherlands) under five stimulation conditions: off stimulation, continuous stimulation, brain stimulation triggered on ipsilateral heel-strike (IHS), brain stimulation triggered on contralateral heel-strike (CHS), and brain stimulation triggered on contralateral toe-off (CTO). There were 4 blocks of 5 conditions each (order randomized within blocks), giving 20 trials in total. One-minute seated rest was provided after each trial and five-minutes seated rest after every 10 trials. Participants wore a safety harness

attached to a sliding overhead support, which prevented falls but was not weight bearing during walking.

Responsive Algorithm

Gait Phase Detection

Gait phase detection was performed in real-time using FSRs (DC:F01 and Trigno 4-Channel FSR Adapter, Delsys Inc, Natick, MA) and accelerometers (Trigno, Delsys Inc, Natick, MA). FSRs were placed between the first and second metatarsal and on the heel to capture changes in ground reaction force (GRF).[172] The change in GRF was converted to a voltage by the FSR ranging from -5 to 0 V. Accelerometers were placed on the shank over the tibialis anterior. Threshold for each FSR was set to 40% of the maximum voltage measured during a short walk on the treadmill. Heel-strike gait phases were detected by the rapid rising segments of the heel FSR voltage and negative acceleration measured on the shank. Toe-off gait phases were detected by the rapid falling segments of metatarsal FSR voltage. Examples of sensor placements, FSR voltage, shank accelerometry, and gait phase detection are illustrated in Figure 9.

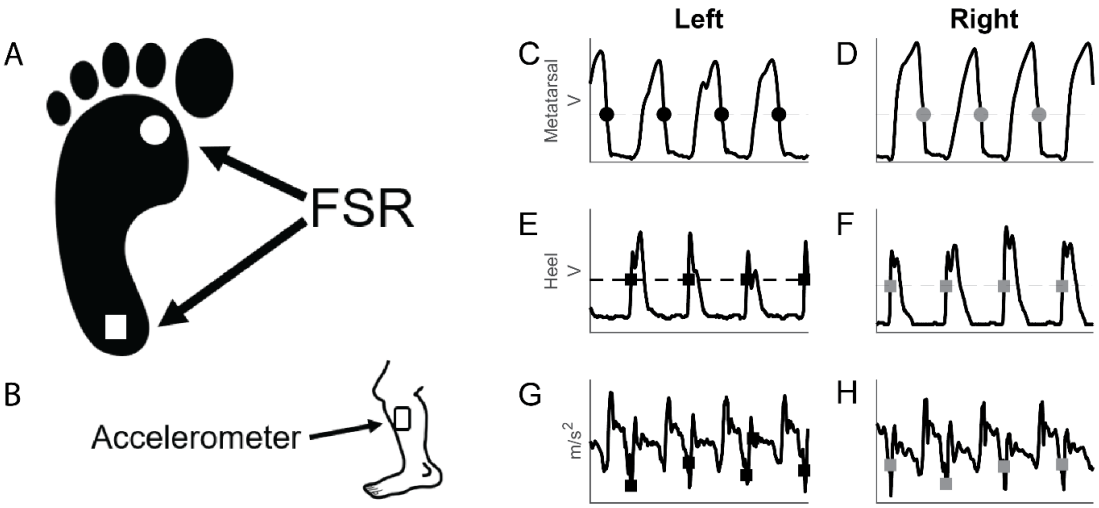

Figure 9. Gait phase detection using force sensitive resistors (FSR) and accelerometers. A) FSRs are placed bilaterally with one sensor between the first and second metatarsal (circle), and the other sensor on the heel of the foot (square). B) Accelerometers were placed on top of the tibialis anterior. C and D), Toe-off gait phases are detected during the rapid falling segments of metatarsal FSR voltage as it crosses 40% of maximal voltage (dashed line). E and F) Heel-strike was detected during the rapid rising segments of heel FSR voltage as it crosses 40% of maximal voltage. G and H) To improve accuracy of heel-strike detection, acceleration measured on the shank must be negative at the time of FSR heel-strike detection.

Stimulation Delivery

Following detection of a heel-strike or toe-off gait phases, a stimulation request was sent to the participant's INS using the Nexus-D3 interface (Medtronic Inc., Minneapolis, MN) after a calculated controlled delay. The controlled delay was required to deliver stimulation at the proper phase of gait in the *following* gait cycle because of hardware, software, and communication system delays (Figure 10). The sum of delays was called the system delay, D . To calculate the controlled delay, the system delay and the average gait cycle duration, $\bar{X}$, must be estimated. The system delays were given by the manufacturer or was measured to be: 390 ms for gait phase detection, 96 ms for wireless transmission from the sensors, and 110 ms for the participant's INS to respond to the stimulation request. Average gait cycle duration was taken as a moving average of the 5 most recent gait cycle durations to average out fluctuations while allowing for gradual trends:

$$\bar{X}_n = \bar{X}_{n-1}\left(\frac{1}{5}(X_n - \bar{X}_{n-1})\right)$$

where X_n is the current gait cycle duration and $\bar{X}_{n-1}$ is the current average gait cycle duration. From the known delays and average cycle duration, we calculated the controlled delay as:

$$\overline{\mathrm{X_n}}\left(1 + \left\lceil\frac{\bar{X}_n - D}{\bar{X}_n}\right\rceil\right) - D.$$

The stimulation request instructed the participant's INS to deliver a short duration stimulation train lasting 125-135 ms in duration.

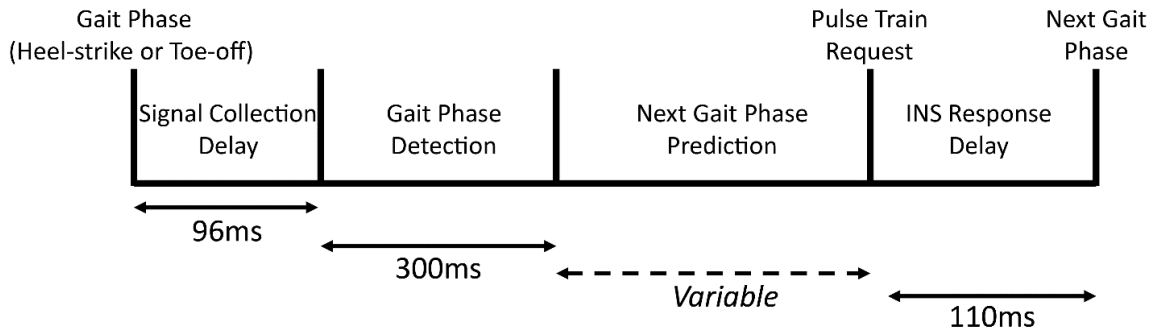

Figure 10. Responsive timing and prediction. A time interval is calculated to delay an INS request for stimulation, such that the short duration pulse trains occur at the next heel-strike or toe-off gait phase. Delays in the system originate from data collection time (96ms), gait phase detection time (300ms), and INS time to respond to a request (110ms).

Data Analysis

Stimulation Delivery Accuracy

Accuracy between stimulation and target gait phase was measured independently of the signals used for rDBS. Gait phases were estimated by the instrumented treadmill (see below: Gait Metrics), and stimulation delivery artifacts were measured using surface EMG sensors on the neck. Left heel-strike was chosen as the start of each gait cycle and was used to determine at what percent of the gait cycle a pulse train was delivered. Mean and standard deviation are reported for each phasic condition. Stimulation artifacts were not detectable with bipolar electrode configuration, therefore gait stimulation accuracy in this configuration was excluded from the analysis.

Gait Metrics

Software supplied by the instrument treadmill manufacturer computed heel-strike and toe-off gait phases from center-of-pressure data measured by a force platform underneath the treadmill belt. We exported time and location of the heel-strike and toe-off gait phases, along with a continuous measurement of the treadmill belt speed to calculate average stride length, stride time, stride width, and double support time using custom Python and MATLAB scripts. Each participant's gait metric was expressed as percent change from the average of no stimulation trials. Analysis of stimulation's effect on each gait metric was done using a separated repeated measures random intercept mixed model with the participant as a random effect. Post-hoc analysis compared off-stimulation to continuous and all phasic stimulation conditions using a t-test. Significance threshold was set at 95% for all analyses. The degree of freedom for all statistical analysis was estimated

using Kenward-Roger's method. Dunnett's adjustment for multiple comparisons was applied following post-hoc analysis.

As our sample was heterogeneous with respect to stimulation target, but we only had 3 GPi participants, we present all participants' data graphically, but focused our statistical analysis on STN participants. Participant 3 (STN) had misplaced leads as determined clinically and by imaging. Data from Participant 3 are presented graphically, in red, but excluded from the statistical analysis.

PD participants may experience a progressive reduction in stride length ("sequence effect")[173,174] which is of particular interest because it may culminate in freezing of gait.[175] To examine this effect in our participants, we first fit a linear regression of stride length against gait cycle, and analyzed the regression slope as a measure of this phenomenon.

Power Analysis

To estimate the study size required to detect significant changes in gait caused by phasic stimulation, we performed a power analysis. We determined the sample size needed to achieve 0.8 statistical power, with an alpha value of 0.05. Power analysis was performed by calculating the percent of significant tests following 200 runs of Monte Carlo simulations for each gait metric and phasic condition. Only STN participants, excluding Participant 3, were considered. For each run, a data set was created by randomly sampling, with replacement, from the available participants' data. Within each participant, four trials for each stimulation condition was randomly sampled with replacement. Post-hoc analysis of a repeated measures linear mixed effect model, with the participant as a random effect,

is used to assess the statistical power. If the power of the model does not reach the power threshold, the data set is increased.

Results

Accuracy of phasic stimulation

Stimulation was delivered accurately during all phasic stimulation trials(Figure 11). Here we report the mean and standard deviation of stimulation delivery as a gait cycle percentage. IHS trials had a mean stimulation delivery occurring at -4.05±9.89% and 52.01±12.56% of the gait cycle. CHS had similar accuracy, with stimulation delivered at -0.38±11.03% and 52.51±11.43% of the gait cycle. CTO stimulation timings had similar spread as IHS and CHS, with stimulation occurring at 16.09±10.37% and 65.93±11.66% of the gait cycle. These percentages correspond with published values of heel-strike and toe-off gait phases.[176]

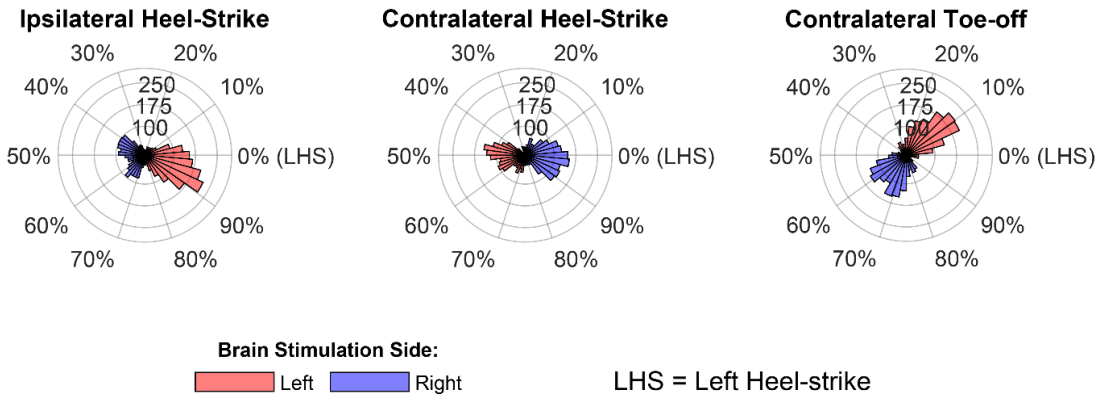

Figure 11. Pulse train delivery as a percentage of gait cycle. The time between the beginning of the pulse train and left heel-strike was calculated for each gait cycle. Polar histograms are shown with 0% indicating left heel-strike.

Phasic stimulation effect on gait

Spatial Metrics

The effect of stimulation condition was significant for both stride length ($F_{(4, 145)}$ = 11.01; $P < 0.01$) and stride width ($F_{(4, 144.88)}$ = 3.51; $P < 0.01$). Post hoc analysis showed this was driven by the continuous stimulation condition. Compared to off stimulation, continuous DBS significantly affected these gait metrics with an average increase of 4.96% in stride length ($t_{(144)}$ = 5.44; $P < 0.01$) and decrease of -4.76% in stride width ($t_{(144)}$ = -2.78; $P = 0.02$), as illustrated in Figure 12 a and b. IHS and CHS phasic stimulation had negligible effects on stride length and width, with an average change of less than 1%. CTO phasic stimulation effect on stride length was also negligible with an average decrease of -0.13%. A larger effect was seen in stride width after CTO stimulation, increasing an average 1.18%. None of the phasic stimulation conditions were significantly different from trials where no stimulation was delivered.

Temporal Metrics

When analyzing temporal gait metrics, stimulation was significant for both stride time ($F_{(4,144.9)}$ = 8.45*;* $P < 0.01$) and double support time ($F_{(4, 144.64)}$ = 8.69; $P < 0.01$). Similar to spatial gait metrics, this was driven by continuous stimulation which significantly affected temporal gait metrics while phasic stimulation did not (Figure 12 c and d). For stride time, continuous stimulation increased the duration by an average of 4.69% of the participant's no stimulation trials ($t_{(144)}$ = 4.64; $P < 0.01$). IHS and CTO slightly increased duration (0.17-0.18%), and CHS decreased duration by -0.42%. These effects were not significant. Double support time increased when the participant's received

continuous stimulation by 4.12% ($t_{(144)} = 5.00$; $P < 0.01$). All phasic conditions increased double support time, but the effect was small (0.20-0.53%) and non-significant.

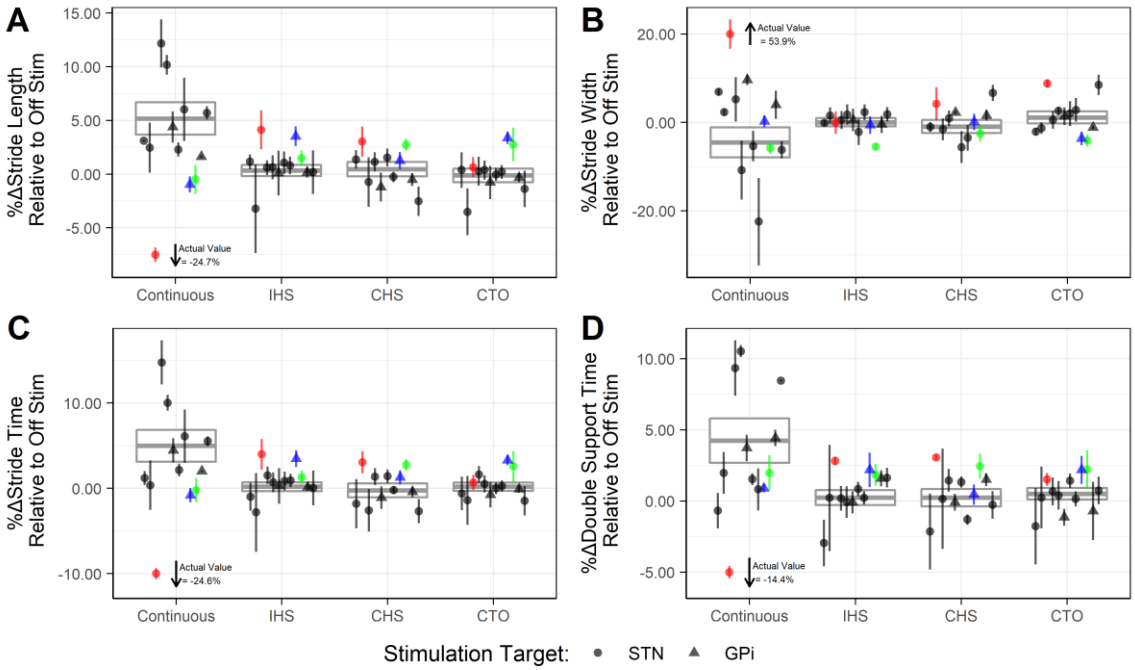

Figure 12. Change in spatial and temporal gait metrics. 9 STN and 3 GPi participants were tested under 5 stimulation conditions, with each condition tested 4 times. Stride length, stride time, stride width, and double support time was calculated for each condition and the percent change, relative to the average gait metric under no stimulation, are shown. Circles are STN participant and triangles are GPi participants. Vertical lines indicate within-subject standard error. Box plots shown are stimulation condition averages and between-subjects standard error of STN participants only. Individuals that responded poorly to continuous stimulation but positively to phasic stimulation are shown in red (Participant 3), blue (Participant 9), and green (Participant 10).

Sequence Effect

Slope of stride length to gait cycle was significantly affected by stimulation ($F_{(4, 144.39)} = 4.26$; $P < 0.003$), shown in Figure 13. Results are similar to spatial and temporal gait metrics, with improved slope observed during continuous stimulation ($t_{(144)} = 2.83$; $P = 0.02$), but not with phasic stimulation. Interestingly, IHS ($t_{(144)} = -0.18$; $P = 0.99$) and CHS ($t_{(145)} = -0.58$; $P = 0.90$) saw a decrease in slope, but increased stride length.

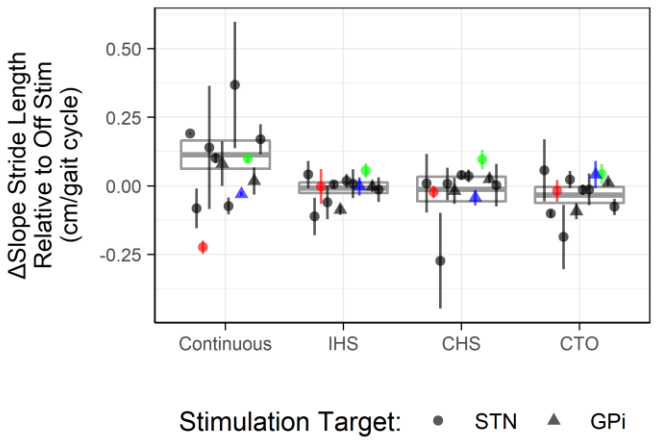

Figure 13. Change in gait cycle slope. The slope of a linear regression between stride length and gait cycle was calculated for each trial and participant. Parkinsonism causes a negative slope, so a positive change in slope means less parkinsonism. Continuous and phasic conditions slopes are shown with respect to no stimulation condition. Box plots represent the stimulation conditions averages and standard error of the mean. Dots and triangles, indicating stimulation target nuclei, represents the mean and standard error of the mean of a participant. Red dot indicates Participant 3, who was excluded from significance testing due to misplaced electrode. Colored data represents individuals that responded positively to phasic stimulation.

Positive responders to phasic stimulation

Three of the participants, two STN and one GPi, showed a *decreased* stride length (0.5-24.7%) and time (0.2-24.6%), i.e. worsening of gait, while receiving continuous stimulation compared to when they received no stimulation (Participant 3, 9, and 10; Figure 12). The same three participants had improved gait while receiving phasic stimulation, i.e. increase in stride length (0.6-4.1%) and time (0.7-4.0%). Double support time saw little change from continuous stimulation in Participants 9 and 10 but was greatly decreased in Participant 3. Stride width also saw small changes in Participant 9 and 10, but a large change in Participant 3 (53.9%).

Power analysis and sample-size estimates

Phasic stimulation caused non-significant changes in spatial and temporal gait metrics. Assuming these non-significant effects were real, we estimated the sample size (number of participants) to achieve 0.8 statistical power for an effect of the observed magnitude, for each gait metric and phasic condition (*Table III*). The lowest estimated sample size across all gait metrics and phases was approximately triple our sample size (26), while the highest was very large at 431 participants. Stride width did not reach significance under IHS phasic stimulation even after Monte Carlo sample sizes reached 1000 participants.

Table III Sample Size Estimates for Gait Phase Modulated DBS

TABLE III
SAMPLE SIZE ESTIMATES

Phase	Stride Length	Stride Time	Stride Width	Double Support Time
IHS	34	61	>1000	26
CHS	52	236	51	212
CTO	35	144	50	431

IHS = Ipsilateral Heel-Strike
CHS = Contralateral Heel-Strike
CTO = Contralateral Toe-Off

Discussion

In this chapter, I demonstrate the feasibility and effect of responsive gait phase triggered DBS on gait in people with PD during treadmill walking. None of the phasic stimulation delivered at specific gait events showed significant changes on gait compared to off stimulation. As expected, I found that continuous DBS did improve all gait metrics measured when compared to gait during off stimulation. This finding allows us to reject the initial hypothesis, that phasic stimulation will be as or more effective than conventional continuous stimulation, and the sample size was large enough to reach this conclusion. If the effect of phasic stimulation at our chosen phases exist, it must be much smaller than the effect of continuous DBS. I estimated sample sizes required to demonstrate such a hypothetical effect, and the range, from best-case to worst-case scenario, was 24 to >1000 participants.

Participants in this study spanned a wide range of UPDRS motor scores, disease duration, and age. Phasic stimulation may only work in a subpopulation of these PD patients. Three participants showed decreased stride length following continuous stimulation, which is an antitherapeutic effect.[148,149,151–154,177–180] Interestingly, in these participants we saw improved gait (increase in stride length) with phasic stimulation. Their UPDRS motor scores ranged from 12-80, disease duration from 6-14, and age from 50-63. Given the wide range of values, this finding suggests that these factors would be poor selectors of patients who would benefit from phasic stimulation. However, we cannot make any conclusions about these factors due to the limited sample size. An alternative approach to select patients for phasic stimulation could be based on whose gait is not improved or is worsened with continuous stimulation (e.g. because of suboptimal lead location). This is

particularly suggested by Participant 3, with sub-optimal lead in the internal capsule. Participants 9 and 10's lead placements are unknown, but the leads may reside in a poor location to treat gait. Previous studies have shown anatomical connections from the dorsal STN to primary motor cortex, supplementary motor cortex and premotor cortex.[9,181] This is the conventional optimal target for stimulation, although this may not be true for gait.[180]

Placing and stimulating the dorsal STN may not be enough for our rDBS algorithm to perform well. The phase of stimulation may not be optimal for their neural circuitry. Local field potential recordings from externalized DBS patients, walking on a treadmill and stepping while seated, showed increases in the alpha-theta band (6-11 Hz)[167] and beta band (13-25 Hz)[168,169] power before and after toe-off and heel-strike gait events. Those studies did not assess inter-individual variation in timing of neural activity modulation during gait. If substantial variation exists, then, in our study, the optimal phase of stimulation might exhibit similar variation. Indeed, the stimulation phase that resulted in the largest increase in stride time and length for Participant 3, 9, and 10 was not the same. Optimal phase might need to be determined on an individual basis for each patient by generating a phase response curve for step or stride length. This method has already been implemented to develop an responsive algorithm to reduce tremor in PD patients.[96]

A limitation in our study is the small sample size. However, it was more than adequate to detect the effect of continuous STN stimulation, and previous aDBS and rDBS studies had similar participant numbers. Another limitation was the small number of participants with GPi DBS, but we observed a similar response to phasic stimulation as in STN participants (that is, increased gait metrics when receiving continuous but not phasic

stimulation, and better response to phasic stimulation in continuous stimulation non-responder).

Another limitation of this study is the short trial durations. Phasic stimulation was only applied for about one minute before changing to another stimulation condition. Phasic stimulation might take longer to reach its full effect. In fact, it takes at least an hour to see the full effects of conventional continuous stimulation on axial symptoms.[67] However, a previous aDBS algorithm study showed changes in beta band power within 100 ms after turning on stimulation, and our algorithm was motivated by endogenous beta modulation during gait. Since our rDBS algorithm relies on stimulation pulse trains lasting 125 ms, we would expect to see a similar effect on beta in our participants.

Another limitation of this study is the amount of energy delivered to the participants. Previous aDBS studies have measured the reduction in total electrical energy delivered (TEED)[145] to the participants. These studies have reported energy reduction between 38-57%.[91,93,94] The approximate energy reduction in our study is between 77-83%, depending on the clinical frequency of the participant and given the duration of the stimulation pulse train. Such a large reduction in energy delivered may explain the small effect sizes we observe. Longer stimulus train durations might have produced larger effects, but would have sacrificed some degree of phase specificity. Also, in this initial study, not knowing what side effects might occur, we opted to err on the side of caution.

In conclusion, we successfully implemented a gait phase triggered rDBS algorithm and demonstrated target engagement. Our results indicate that time-locked stimulation to heel-strike and toe-off gait phases did not improve gait parameters to the same degree as continuous stimulation. Stimulation at other phases may be more effective but were not

tested. In a finding that was suggestive, the benefit of phasic stimulation may be larger in patients for whom continuous stimulation is ineffective, e.g. when lead location is suboptimal by conventional criteria.

Chapter 4 – STN DBS Effects on Parkinsonian Gait are Detectable Without Prolonged Wash- in/out

Introduction

Parkinson's disease (PD) deep brain stimulation (DBS) literature includes a large number of studies which assess the effects of stimulation by measuring symptoms in the ON- vs OFF-stimulation condition. It is known that subthalamic DBS effects on PD symptoms wash-in and out gradually.[67,68] The wash in and out effects of pallidal stimulation on symptoms has not been studied, but have been assumed to be similar to subthalamic stimulation. This assumption was used in a major clinical trial design to allow at least 1 hour of wash in and out for both targets.[40,182,183] A drawback of this long of a washout period is that, typically, only a single stimulation setting can be assessed in a visit: the patient's "clinical" stimulation settings, i.e. those established by the treating clinician and stable for months prior to the measurements.

For studies that assess multiple settings, a wash-out period shorter than 1 hour is needed. For some motor symptoms a shorter wash-out period is well established. The influential paper of Temperli et al. is often cited to support the chosen wash-out period for the motor symptom under study.[67] For the motor symptom of tremor and bradykinesia, the wash-out period can be as short as 30 minutes. Whereas axial symptoms were reported by Temperli et al. to take over an hour for stimulation to wash-out. Gait is an axial symptom, and studies that examine stimulation’s effect on gait should implement a wash-out period *at least* 1 hour in duration. In practice, this is often hard to achieve, and shorter intervals are common in the literature.[180,184] Moreover, if the experiment implements a 1-hour washout period, stimulation cannot be turned on/off repeatedly in the same experiment day; such within-subject replication requires multiple days of experiments.

Recently, we conducted a series of experiments in which we compared the effects on gait of three different novel DBS settings (gait phase modulated DBS), with multiple within-subject replications. In addition to the novel DBS settings, we included two control settings: the participant's clinical settings and a no stimulation setting. In order to make multiple gait measurements, we did one full wash-out at the beginning of the experiment, but between different settings we only provided 1-minute of wash-out time, which we term a "hyperacute" protocol. Results of the gait phase modulated stimulation are reported elsewhere, but the paper only evaluated the novel stimulation settings in the hyperacute protocol (Chapter 3 - Results). In short, the findings were that the novel DBS stimulation locked to gait were delivered accurately, but the stimulation did not improve gait. Despite the lack of wash- in/out, the therapeutic effects captured with the hyperacute protocol on multiple gait metrics were quite robust. This suggests that DBS gait effects can successfully be measured with a hyperacute protocol.

The success of the hyperacute protocol was somewhat surprising in light of the reported slow wash- in/out of axial symptoms.[67] It suggests that after DBS is turned off, some portion of the total therapeutic effect on gait disappears immediately, and the remainder washes out gradually, as we previously reported for bradykinesia.[68] To assess if the immediate effect is comparable to the effect seen during a full wash-out period, we present previously unpublished data and analysis from the gait phase modulated DBS trial. The full wash-out period done prior to the hyperacute protocol measured gait at the start of the period, with stimulation ON, then again immediately after turning off stimulation (Acute OFF), and again after minimum 1 hour (Late OFF). We measure the effect of wash-out time on gait, and then we compare the two time points to see how much of the total

therapeutic effect washes out immediately. Afterwards, the hyperacute effect, measured for the two control conditions, is compared to the total therapeutic effect observed at Late OFF in the wash-out period. Lastly, we estimate the minimal sample sizes for the hyperacute and wash-out protocol to detect an effect.

First, we found that DBS gait effect measured in this way corresponded well to DBS gait effect measured in the hyperacute protocol, confirming that both protocols measured the same effect. Next, we found that, when comparing ON to Late OFF (full washout), DBS gait effect was consistently significant, whereas comparing ON to Acute OFF, the effect, though in the same direction, was weaker and did not consistently reach statistical significance. In agreement with this, a direct comparison of Acute OFF to Late OFF gait effect showed that the Acute OFF effect was about 49% smaller than the Late OFF effect, i.e. about 49% of the therapeutic effect disappeared immediately, leaving the remaining half to wash out gradually. Finally, we estimated a minimal sample size for the full-washout protocol and compared it to the required size for the hyperacute protocol. We found that the hyperacute protocol requires a lower sample size, compared to the full-washout protocol, to detect stimulation's effect on gait.

Methods

Participants

Fourteen PD individuals with bilateral STN DBS leads and Medtronic SC, PC, or RC implantable neural stimulators (INSs) (Medtronic Inc., Minneapolis, MN) participated in the study (*Table IV*). A subset of the data was shown previously (Chapter 3 - Results). Participants were tested after overnight withdrawal of PD medication prior to the study.

All participants gave informed consent according to a University of Minnesota Institutional Review Board approved protocol.

Table IV Participant Demographics for Chapter 4

TABLE IV
PARTICIPANT DEMOGRAPHICS

Participant	1	2	3	4	5	6	7	8	9	10	11	12	13	14
Age	59	56	65	64	52	72	67	64	61	79	83	58	63	39
Sex	M	M	M	M	F	M	F	M	M	M	M	F	M	F
Disease Duration	13	19	26	13	12	6	12	8	18	4	10	24	6	9
Gait Speed Overground (m/s)	0.87	0.31	0.65	0.45	0.65	0.80	1.00	0.55	1.39	1.18	1.08	1.47	1.15	1.10
Gait Speed Treadmill (m/s)	0.87	0.23	0.42	0.23	0.49	0.80	1.00	0.55	1.39	1.18	1.08	1.47	1.15	1.10
Stimulation Target	STN	STN	STN	STN	STN	STN	STN	STN	STN	STN	STN	STN	STN	STN
MDS-UPDRS III														
Total	27	64	37	70	68	35	24	58	19	41	37	31	12	56
Clinical Settings														
Contacts														
Left	c+2-	2+3-	c+1-2-	1+0-	c+1-	c+2-	3+2-	c+1-2-	c+1-	c+1-	c+3-	3+1-2-	c+1-	c+2-
Right	c+1-	c+2-	c+5-	c+0-	1+0-	c+9-	c+10-	c+11-	c+1-	c+3-	c+2-	c+6-7-	3+1-	c+10-
Amplitude														
Left	2.8 V	2.5 V	3.2 V	2.8 V	0.5 V	1.4 mA	3.4 V	3.6 V	2.2 V	2.5 V	3.0 V	3.2 V	2.9 V	2.9 V
Right	3.9 V	2.8 V	3.2 V	2.6 V	1.5 V	2.0 mA	2.9 V	2.0 V	2.5 V	2.5 V	3.8 V	3.0 V	3.1 V	2.9 V
Frequency (Hz)														
Left	130	185	160	130	130	130	130	200	130	130	130	130	130	150
Right	130	185	160	130	130	130	130	200	130	180	130	130	130	150
Pulse Width (μs)														
Left	60	60	60	60	60	60	80	120	60	60	60	70	60	60
Right	60	60	60	90	90	60	70	90	60	90	60	70	60	60
Experimental Settings														
Contacts														
Left	c+2-	c+3-	c+1-2-	c+1-	c+1-	c+2-	3+2-	c+1-2-	c+1-	c+1-	c+3-	3+1-2-	c+1-	c+2-
Right	c+1-	c+2-	c+5-	c+0-	c+1-	c+9-	c+10-	c+11-	c+1-	c+3-	c+2-	c+6-7-	3+1-	c+10-
Amplitude														
Left	2.5 mA	2.7 mA	3.0 mA	2.0 mA	0.4 mA	1.4 mA	3.5 mA	3.6 mA	3.0 mA	3.0 mA	2.5 mA	3.0 mA	2.5 mA	2.7 mA
Right	3.6 mA	3.1 mA	3.0 mA	2.5 mA	1.0 mA	2.0 mA	3.0 mA	2.0 mA	3.0 mA	3.0 mA	3.5 mA	3.0 mA	1.6 mA	2.5 mA

STN = Subthalamic Nucleus

Experimental Protocol

Gait was first measured overground 20 ft in a hallway 12 times at a self-selected speed. Gait was then measured on an instrumented treadmill (C-Mill, MotekforceLink, Netherlands) in two protocols: washout and hyperacute. The washout protocol was conducted prior to the hyperacute protocol and consisted of gait measurements ON-DBS, immediately after turning off DBS (Acute OFF), and after a minimum of 1 hour off DBS (Late OFF). Since we are measuring gait after at least 1-hour off stimulation and then in the hyperacute protocol, we considered the possibility that the participant would no longer be able to walk at their overground speed. In order to have at least one treadmill speed common throughout protocols, we tested three percentages of the participants overground speed at each time point in the washout protocol: 100, 85, and 75%. Two trials ON DBS at 100% was tested to account for participants who have not been on a treadmill in a year. In three participants we also tested 65% of their overground speed, with one of these participants having an additional test at 50%. Participant 3 only tested at 65% of their overground speed during Late OFF as they had great difficulty walking on the treadmill at 75%. Each trial lasted one minute. The fastest overground speed percentage that the participant could tolerate was set for all gait measurements during the hyperacute protocol.

The testing procedure and changes to participant's stimulation settings in the hyperacute protocol was previously described in Chapter 3 - Experimental Protocol.

Data Analysis

Gait Metrics

Software supplied by the instrument treadmill manufacturer computed heel-strike and toe-off gait phases from center-of-pressure data measured by a force platform underneath the treadmill belt. We exported time and location of the heel-strike and toe-off gait phases, along with a continuous measurement of the treadmill belt speed to calculate average stride length, stride time, stride width, double support time, and cadence using custom Python and MATLAB scripts.

Statistical Analysis

We examined the effects observed during the washout and hyperacute protocol through in three parts. First, we analyzed the effect of washout time on gait measured at all three time points during the washout protocol. This analysis grouped all participants together into a separated repeated measures random intercept mixed model with the time point (ON, Acute OFF, and Late OFF) and treadmill speed (100, 85, 75, 65, or 50% of ON-overground speed) as categorical fixed effect and the participant as a random effect. The inclusion of all treadmill speeds was to make use of additional data. In addition to the linear model, a post-hoc analysis compared ON to Acute OFF and Late OFF using a t-test. Second, we directly compare the effect seen at Acute OFF and Late OFF. To start this analysis, a linear model was created for each participant with washout time point and treadmill speed as fixed factors. From this model we obtained the effect size and associated standard error at each time point for each participant. Then, the effect sizes at the two time points are entered into a linear regression, and the r-squared value and slope are reported. Third, we directly compare the effect at Late OFF to the effect seen during the hyperacute protocol. Analysis steps are identical to the second analysis, but the linear model and

regression replaces the Acute OFF data with the hyperacute data. Participant 3 was excluded from the third analysis because the speed tested during the hyperacute protocol was only tested at Late OFF in the washout protocol. Significance threshold was set at 95% for all analyses. The degree of freedom for all statistical analysis was estimated using Kenward-Roger's method. Tukey's adjustment for multiple comparisons was applied following post-hoc analysis.

Power Analysis

We performed a power analysis to estimate the study size required to detect significant changes in gait between ON to Late OFF DBS washout and hyperacute OFF to ON stimulation. We determined the sample size needed to achieve 0.8 statistical power, with an alpha value of 0.05. Power analysis was performed by calculating the percent of significant tests following 200 runs of Monte Carlo simulations for each gait metric. For each run, a data set was created by randomly sampling, with replacement, from the available participants' data. Within each participant, two trials of ON DBS at 100% was randomly sampled with replacement when estimating the sample size between ON to Late OFF. All other time points and overground speed percentages were taken. Similarly, when estimating the sample size between hyperacute OFF to hyperacute ON four trials were randomly sampled with replacement. Post-hoc analysis of a repeated measures linear mixed effect model, with time point and treadmill speed as fixed effects and participants as a random effect, is used to assess the statistical power. If the power of the model does not reach the power threshold, the number of participants is increased.

Results

Gait metrics were measured across two protocols: washout and hyperacute. The washout protocol measured gait metrics at three time points and at different percentages of the participant's overground walking speed. The three time points during the washout protocol are at the beginning, with stimulation ON, immediately after turning off stimulation (Acute OFF), and after a minimum of 1 hour (Late OFF). At each time point the speed of the treadmill was set to 100, 85, and 75% of the participant's overground walking speed. Three participants had additional speeds tested below 75%. The hyperacute protocol measured gait metrics under 5 stimulation conditions with very little wash-in or wash-out of DBS effects. Relevant to this paper, we analyzed only two control conditions from the hyperacute protocol, the participants' clinical settings (hyperacute ON) and compared that to no stimulation delivered (hyperacute OFF). We report on the change in gait metric at different time points during the washout protocol, compare gait metric changes during washout, and compare gait changes at Late OFF to the hyperacute control conditions.

Washout protocol gait effects

Increases and decreases for all gait metrics are seen at Acute OFF (Figure 14). For most participants across most treadmill speeds, stride time, stride width, and double support time was decreased. Stride length and cadence did not show a favored response, with similar number of participants and treadmill speeds that increased and decreased. Following a minimum of 1-hour wash-out, Late OFF sees more participants and treadmill speeds that are decreased for stride length and stride time (Figure 15 A and B) and increased

cadence (Figure 15 E). These changes were detected in our linear mixed effect model, where the washout duration was a significant factor (*Table V*). Post-hoc analysis confirmed that Late OFF was the driving force for significance of stride length, stride time, and cadence.

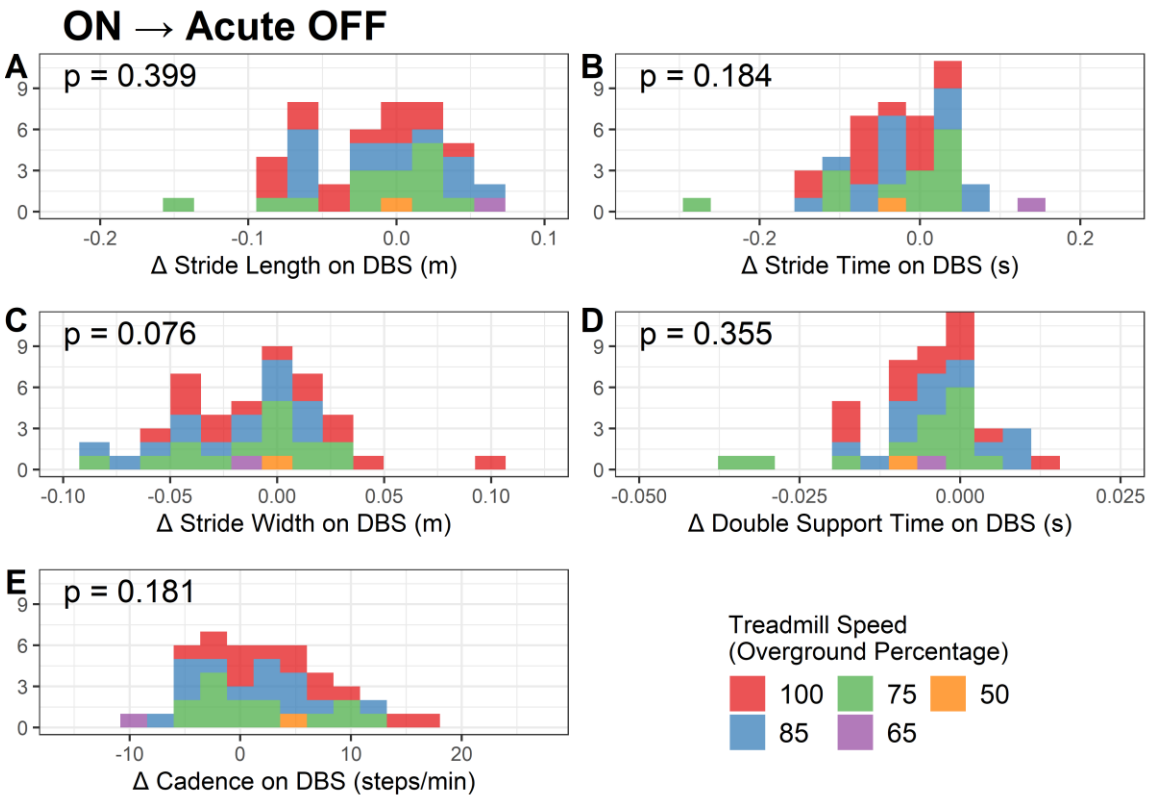

Figure 14. Histogram of gait effects measured immediately after turning off stimulation. Stacked histograms of the change in gait metrics from ON DBS to Acute OFF. Each color represents the treadmill speed as a percentage of overground walking speed that a participant was tested under. Post-hoc p-values were calculated using a t-test on the results of the linear mixed effect models and are shown in each graph. No gait metric was significantly changed when measured at Acute OFF compared to ON-stimulation.

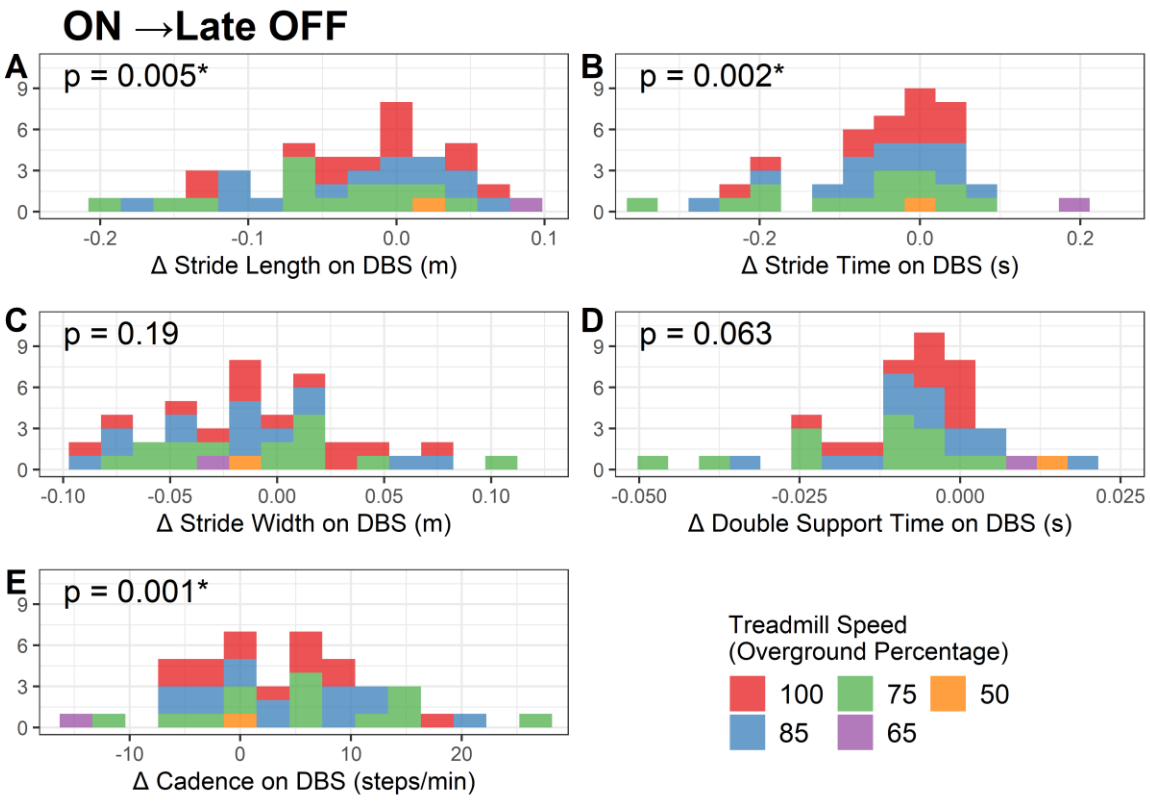

Figure 15. Histogram of gait effects measured after minimum 1-hour after turning off stimulation. Stacked histograms of the change in gait metrics from ON DBS to Late OFF. Each color represents the treadmill speed as a percentage of overground walking speed that a participant was tested under. Post-hoc p-values were calculated using a t-test on the results of the linear mixed effect models and are shown in each graph. Significance was set to $p<0.05$ and is denoted by "*".

Table V Statistical Analysis Results of Gait Effect in a Washout Protocol

TABLE V
STATISTICAL ANALYSIS

	Stride Length	Stride Time	Stride Width	Double Support Time	Cadence
F-statistic	$F_{(2,144.02)} = 5.08$ **p = 0.007**	$F_{(2,144.22)} = 6.21$ **p = 0.003**	$F_{(2,144.06)} = 2.76$ p = 0.07	$F_{(2,144.12)} = 2.66$ p = 0.07	$F_{(2,144.22)} = 6.45$ **p = 0.002**
Post-hoc t-test					
Acute OFF	$t_{(144)} = -1.30$ p = 0.399	$t_{(144)} = -1.77$ p = 0.184	$t_{(144)} = -2.19$ p = 0.076	$t_{(144)} = -1.38$ p = 0.355	$t_{(144)} = 1.78$ p = 0.181
Late OFF	$t_{(144)} = -3.18$ **p = 0.005**	$t_{(144)} = -3.52$ **p = 0.002**	$t_{(144)} = -1.75$ p = 0.19	$t_{(144)} = -2.27$ p = 0.063	$t_{(144)} = 3.59$ **p = 0.001**

DF estimated using Kenward-Roger's method
p-value adjusted using Tukey's method

Comparison between Acute OFF and Late OFF, using a linear model, indicates that stride length, stride time, stride width, and cadence are approximately linear. The r-squared values for these metrics are 0.694, 0.740, 0.614, and 0.612 for stride length, stride time, stride width, and cadence respectively (Figure 16 A, B, C, and E). Double support time is poorly approximated by a linear trend, obtaining an r-squared value of 0.381 (Figure 16 D). The linear models shown here predicted the Acute OFF effect from the Late OFF effect. This means that the slopes of the linear models allow us to approximate, on average, how much of the effect size washes out immediately. Acute OFF's effect on stride length, stride time, stride width, and cadence were approximately 52, 52, 58, and 51% of Late OFF effect, respectively. Double support time Acute OFF effect was smaller than other gait metrics, only reaching 34% of the Late OFF effect. Interestingly, a few participants Acute OFF gait effect was the same as their Late OFF effect. This is seen for all gait metrics and are the points that lie on the identity line (dashed line) in Figure 16.

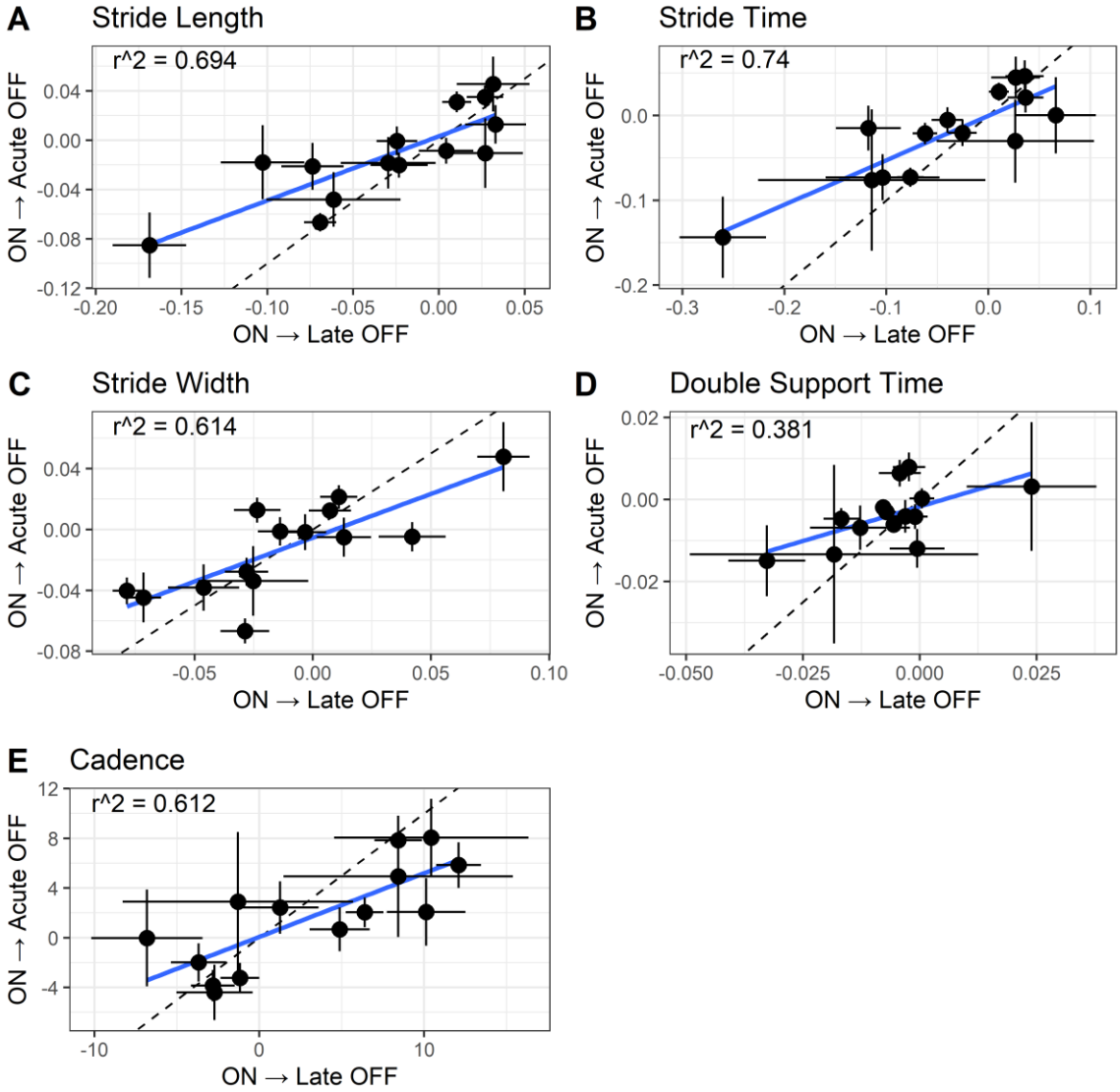

Figure 16. Comparison between gait effects seen at Acute OFF and Late OFF. Scatterplots of Acute OFF and Late OFF gait effect. Points and bars indicate mean and standard error of a participant's change in gait metric. Regression between Acute OFF and Late OFF is shown as the solid blue line. Dashed line indicates the identity line, where the effect on gait at Late OFF is the same as at Acute OFF. R-squared values are shown in the top left corner of each plot. Color indicates participants whose electrode configuration changed for the hyperacute protocol.

Hyperacute gait effects

The gait effect relationship between Late OFF and the hyperacute interval is comparable to the relationship between Acute OFF and Late OFF. Stride length, stride time, and cadence are moderately linear, with r-squared values of 0.528, 0.506, and 0.440 respectively (Figure 17 A, B, and E). However, stride width and double support time is poorly described by a linear approximation and is reflected in the low r-squared values (Figure 17 C and D). Although r-squared values were lower for all gait metrics, stride length, stride time, and cadence's slope were similar to what was observed during the washout protocol. For these gait metrics, the slope was 46%, 43%, and 54%, respectively. This indicates that the hyperacute protocol captured approximately 48% of the Late OFF effect for these gait metrics, which is comparable to the effect seen at Acute OFF. Stride width and double support time, under the hyperacute protocol, was only able to capture 35% and 29% of the Late OFF effect.

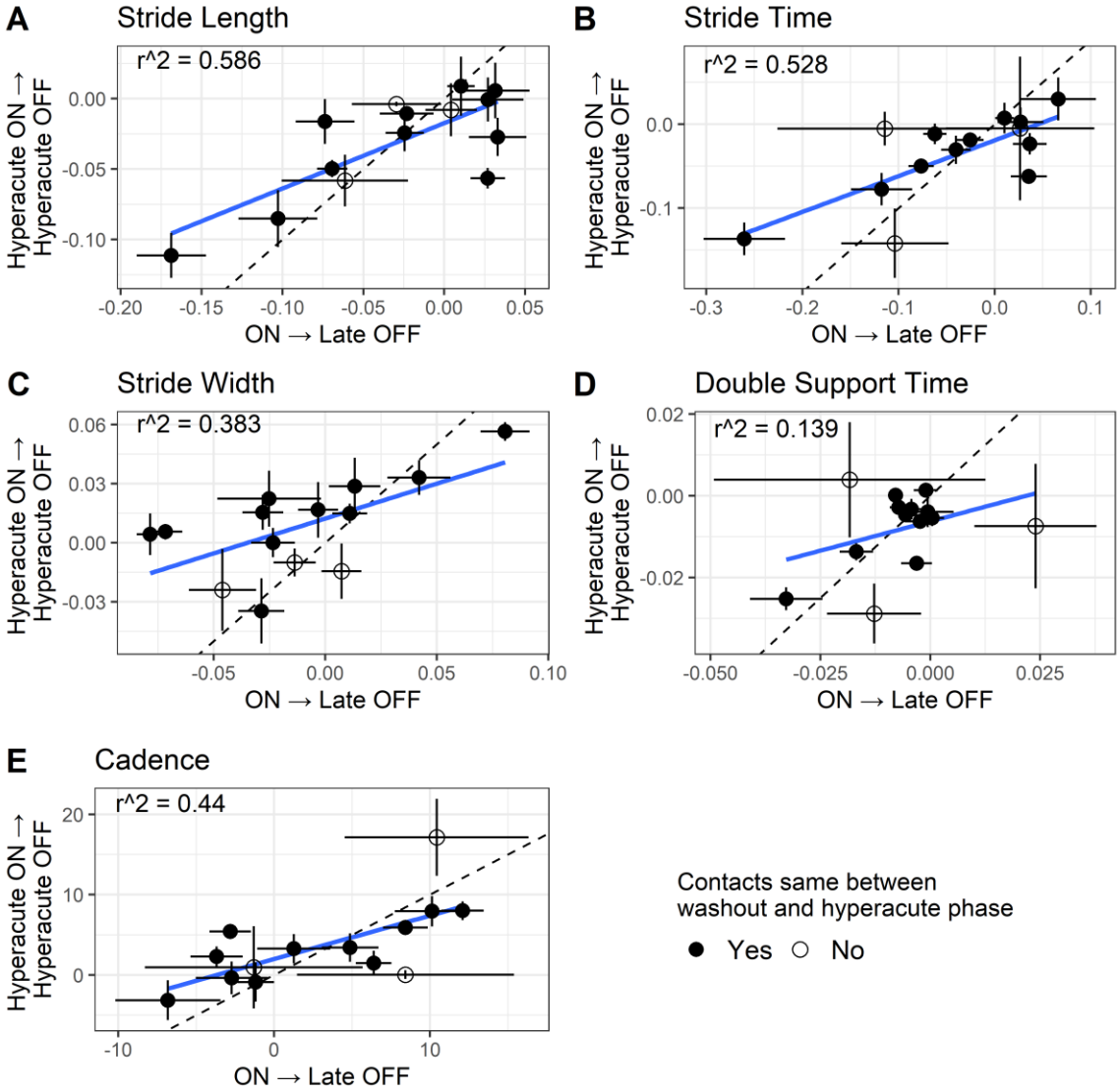

Figure 17. Comparison between gait effects measured with the hyperacute protocol and Late OFF (full washout). Scatterplots of comparing gait effect seen with the hyperacute protocol and Late OFF. Points and bars indicate mean and standard error of a participant's change in gait metric. Filled and open circle indicate if the participant's contacted were changed for the hyperacute protocol. Regression between hyperacute protocol and Late OFF is shown as the solid blue line. Dashed line indicates the identity line, where the effect on gait at Late OFF is the same as the hyperacute protocol. R-squared values are shown in the top left corner of each plot.

Power analysis and sample size estimates

Significant effects on gait is seen after a minimum 1-hour washout. However, a non-significant change in gait is seen immediately turning off stimulation. The hyperacute protocol tested was able to capture gait effects that corresponds well to the immediate washout effect, indicating the hyperacute protocol is measuring the same effect. We estimated the number of participants to achieve 0.8 statistical power for each gait metric under a hyperacute protocol and washout protocol (*Table VI*). Sample size estimates for the hyperacute protocol ranged from 5-38 participants, while Late OFF ranged from 15-37 participants. For a majority of the gait metrics measured, the estimated sample size needed to detect an effect was smaller than amount needed under the washout protocol.

Table VI Sample Size Estimates for a Washout and Hyperacute Protocol

TABLE VI
SAMPLE SIZE ESTIMATES

Interval	Stride Length	Stride Time	Stride Width	Double Support Time	Cadence
ON → Late OFF	15	18	37	22	18
Hyperacute ON → Hyperacute OFF	5	9	38	7	8

Discussion

In this chapter, I compare STN DBS effect on gait during treadmill walking in two protocols: full washout and hyperacute. In the full washout protocol, I found that when comparing ON stimulation to Late OFF, DBS gait effect was consistently statistically significant. However, when comparing ON to Acute OFF, the effect, though in the same direction at Late OFF, did not consistently reach statistical significance. In agreement with this, a direct comparison of Acute OFF to Late OFF gait effect showed that the Acute OFF effect was about 49% smaller than the Late OFF effect, i.e. about 49% of the therapeutic effect disappeared rapidly, leaving the remaining half to wash out gradually. This is an average over patients, but the proportion of rapidly-disappearing gait effect varied among patients, as seen in a previous study of DBS effects on bradykinesia.[68]

When comparing the effect on gait in the hyperacute protocol to Late OFF, the effect seen in the hyperacute protocol was 41% smaller, but well-correlated with it. We estimated the number of participants (sample size) needed to detect an effect at Late OFF with hyperacute protocol and the full washout. Across a majority of gait metrics, fewer participants are needed to detect an effect in the hyperacute protocol compared to the full washout protocol. Even though the error was greater on a single trial using the hyperacute protocol, the repeated measures allowed the standard error to be smaller. This could reflect the close temporal proximity of the measurements compared in contrast to the washout protocol: the prolonged wait for washout may have introduced unmeasured confounders which functioned, collectively as noise or non-stationarity. The hyperacute protocol also reduced variance by replicating the DBS ON → OFF transition four times in each subject, whereas only a single transition was feasible in the washout protocol.

Temperli et al. measured changes in motor symptoms at various durations of washout.[67] Their data showed axial symptoms require over an hour to reach 90% of maximum washout but this is rarely feasible and washout is often briefer in practice. Although they do not directly address this issue, figures suggest that washout of axial symptoms may be initially rapid (short time constant) followed by a slower washout (longer time constant), a pattern previously reported for bradykinesia.[68] The axial subscore presented by Temperli et al. includes multiple symptoms, including gait, and it is currently unknown if gait contributes more to the initial fast, or to the later slow washout seen in their figures, or to both. Our data suggests both. Indeed, the percentage of total washout on gait at Acute OFF is similar to the 5-minute time point in their data. Regardless, our data replicated their finding that complete washout of gait effect requires least one hour.

The presence of a fast and slow phase of gait washout may indicate differences in stimulation locations within the STN. In a previous study, we found return of bradykinesia after cessation of STN stimulation[68] had both a fast and slow wash-out phase, and the location within the STN region determined their relative magnitudes. In the data presented in this study, some participants' gait effect completely washed-out when measured at Acute OFF (Figure 16, points on the identity line), indicating that almost all the detectible effects of DBS washed out in the fast phase. While we do not know the location of the electrode relative to the STN in our participants, the finding from our previous study suggests that differences in DBS implant location may explain these differences.

Our study uses data from experiments undertaken for a different experiment (to test gait phase modulated DBS). Consequently, A few of our participants whose clinical settings, in the washout protocol were bipolar, had their clinical settings approximated with

pseudomonopolar settings. This is previously described in Chapter 4 - Experimental Protocol. Nonetheless, stride time, stride width, double support time, and cadence were all well-correlated between hyperacute and washout protocols, and the participants changed to monopolar do not deviate from this pattern, except, possibly, for double support time.

Another limitation related to our use of data from the gait phase modulated DBS study is that, in addition to the ON vs. OFF settings reported here, novel stimulation settings were also tested in the hyperacute protocol. Conceivably, the novel stimulation may have had some indirect, carry-over effect on the ON vs OFF stimulation gait effect we report here. If so, the effect was to amplify the effect of conventional stimulation, which would be remarkable. However, this is unlikely as the direct effect of the novel gait phase modulated stimulation was small and nonsignificant.

Another limitation of the study is that the washout interval, though never shorter than one hour, did vary among participants. Five started the hyperacute protocol after 120-minutes off stimulation, whereas all other participants started before 90-minutes had passed. It has been reported that axial symptoms do not significantly change after 90-minutes of washout compared to 60-minutes, but 120-minutes is significantly different.[67] Moreover, the comparison between Acute OFF and Late OFF is similar to what has been seen previously.[67]

In conclusion, the results in this chapter suggests both a fast and slow phase of stimulation washout in gait. The effects of stimulation on the hyperacute phase and the full-washout are similar enough that the hyperacute phase may be used to test different settings. I propose that multiple testing of stimulation using a hyperacute protocol rather than a

single trial using the full washout may have higher sensitivity to stimulation setting effects and may achieve significant effects with fewer subjects for most motor symptoms.

Chapter 5 – Conclusions

The overall goal of this thesis is to investigate the use of quantified motor behavior to develop and improve deep brain stimulation (DBS) therapy for Parkinson's disease (PD). Specifically, this work has provided a framework for using quantified motor behavior to advance DBS therapy by: 1) providing proof-of-principal evidence on the use of Bayesian optimization for stimulation parameter optimization; 2) demonstrating feasibility of state specific real-time stimulation based on gait to treat motor behavior; and 3) providing evidence that gait changes due to stimulation parameter changes measured during short duration wash-in and out of results in similar findings as when a full wash-out interval is used. This work demonstrates how quantified motor behavior enables closed-loop approaches to improve DBS therapy.

Summary and Significance of Results

Deep brain stimulation is a therapy used to treat the motor signs of patients with Parkinson's disease. Following lead implantation, stimulation parameter optimization is performed by a clinician using a trial-and-error process.[76] This can take 50 or more hours before sufficient alleviation of motor signs and minimal side effects is achieved.[75] Motor sign improvements between 20-50% are seen following parameter optimization.[31–33] However, gait is not considered to be adequately treated.[158] In this thesis, I propose using quantified motor behavior to improve DBS outcomes. This approach has the potential to reduce time spent tuning stimulation parameter, improve therapeutic outcomes of stimulation, and improve study designs.

Using Quantified Motor Behavior Outcomes to Optimize Stimulation for DBS

Quantified motor behavior could be used with currently available implantable neural stimulators in PD patients to optimize stimulation parameters. This approach was successfully used to quickly and accurately optimize frequency to reduce forearm rigidity in Chapter 2 – Semi-Automated Approaches to Optimize Deep Brain Stimulation Parameters in Parkinson's Disease. Other motor signs and stimulation parameters can be added easily to this method. Optimization time using a Bayesian optimization approach will increase as more factors are optimized, but the increase the time of optimization would be short compared to a trial-and-error approach. This is particularly true with the increasing availability of segmented electrode designs that increase the number of electrodes from 4 to 8.

It is likely that stimulation settings would need to be changed as the disease progresses. Re-optimizing stimulation parameters with this approach can account for this change. Instead of a assuming no prior information on the response of motor signs to stimulation parameters, the patient's previous optimization data can be used as a priori information into the Bayesian optimization algorithm. This would allow for quick adjustments of stimulation parameters as the disease progresses.

Using Quantified Motor Behavior Outcomes for Development of Novel Stimulation Approach

Neural stimulators have been developed that can simultaneously record and stimulate. This sensing technology has been used to developed novel stimulation therapy approaches that continuously adjust the stimulation amplitude.[90,91] There are many

advantages to these novel approaches: 1) they achieve similar or improved efficacy, 2) they reduce power consumption, and 3) reduce side effects associated with stimulation.

In Chapter 3 – Gait Phase Triggered Deep Brain Stimulation in Parkinson's Disease, a novel stimulation delivery approach to treat gait was proposed. The approach triggered stimulation, timed to heel-strike and toe-off gait phases, for 125-135 ms. Stimulation delivered at these gait phases was effective at improving gait for a small subset of the participants, providing evidence that using quantified motor behaviors to trigger stimulation can improve stimulation outcomes. For the other participants, the gait phases stimulation is triggered on may not be optimal. Instead of setting which gait phases to trigger stimulation, a phase response curve could be added to the approach that would determine the optimal gait phase to stimulate.

It is possible that the hyperacute protocol implemented in Chapter 3 – Gait Phase Triggered Deep Brain Stimulation in Parkinson's Disease, i.e. 1-minute of wash-in and wash-out time between stimulation conditions, was not sufficiently long enough to see an effect of this novel stimulation approach. Chapter 4 – examined the hyperacute protocol and compared stimulation's effect on gait with a 1-hour wash-out protocol. This duration of washout is commonly implemented in studies examining stimulation's effect on gait. I found that the effect measured using the hyperacute protocol was comparable to the 1-hour wash-out protocol. This implies that the hyperacute protocol can be used to test multiple stimulation settings in a single visit. Future studies that wish to examine multiple stimulation settings may implement the hyperacute protocol without significant loss of sensitivity.

Limitations

Here I propose the use of quantified motor behavior outcomes to improve DBS for PD. However, there are number of potential issues when measuring motor behavior. 1) Specific placement of sensors was required to successfully implement the novel gait phase stimulation delivery approach. If the sensors were placed in suboptimal locations, the sensors would not have sensed the changes in foot pressure necessary to detect the beginning of heel-strike and toe-off. A study on foot pressure distributions during gait showed that peak pressure at the 4th and 5th metatarsal is less than half of what is seen between the 2nd metatarsal.[172] Additionally, the study showed that pressure *near* the heel, towards the toes, does not show an immediate increase in pressure during heel-strike. Sensor placement is crucial to correctly quantify the motor behavior outcome under study. 2) When quantifying a motor behavior outcome, other movements can influence the value. It has been reported by Powell et al. that contralateral movements increases rigidity in Parkinson's disease in the off medication state.[185] The same study showed that contralateral activation increased rigidity in the on medication state, but was it was not significant. It is unknown how other parkinsonian motor signs are affected with other movement. With regards to the stimulation parameter optimization approach suggested in this thesis, other movements that occurs while measuring rigidity would decrease sensitivity and therefore decrease the ability to optimize the settings. To account for this, additional tests at the stimulation setting could be conducted until other movements are averaged out. 3) Injury to the body could alter the motor behavior measurement. PD patients are at a higher risk for falls than other neurological conditions and are more likely to have recurrent falls.[186,187] If a PD patient experiences a fall, they may experience musculoskeletal pain and previous

studies have reported that musculoskeletal pain alters muscle activation and control.[188] This suggests that the motor behavior measurements are not representative of only Parkinson's pathology.

Conclusion

While there are many approaches to improve DBS outcomes in PD[77–80,90,91,96], each technique need to be validated. Quantified motor behaviors offer an alternative approach to build tools and methods to improve DBS outcomes in PD. The approach generates a flexible signal that can be used in a variety of applications, such as parameter optimization or novel stimulation delivery. Furthermore, quantified motor behaviors can be used to justify future study design choices where multiple stimulation settings want to be tested in a short duration. The use of quantified motor behaviors to develop tools and methods has the potential to improve stimulation's efficacy and thereby improving the patient's quality of life.

References

1. Bertram, L., Bertram, L., Tanzi, R. E. & Tanzi, R. E. The genetic epidemiology of neurodegenerative disease. *J. Clin. Invest.* **115**, 1449–1457 (2005).
2. Tysnes, O.-B. & Storstein, A. Epidemiology of Parkinson's disease. *J. Neural Transm.* **124**, 901–905 (2017).
3. Marras, C. *et al.* Prevalence of Parkinson's disease across North America. *npj Park. Dis.* **4**, 1–7 (2018).
4. Poewe, W. Non-motor symptoms in Parkinson's disease. *Eur. J. Neurol.* **15 Suppl 1**, 14–20 (2008).
5. Braak, H. *et al.* Staging of brain pathology related to sporadic Parkinson's disease. *Neurobiol. Aging* **24**, 197–211 (2003).
6. Spillantini, M. G. *et al.* Alpha-synuclein in Lewy bodies. *Nature* **388**, 839–40 (1997).
7. Gibb, W. R. & Lees, A. J. Anatomy, pigmentation, ventral and dorsal subpopulations of the substantia nigra, and differential cell death in Parkinson's disease. *J. Neurol. Neurosurg. Psychiatry* **54**, 388–96 (1991).
8. Damier, P., Hirsch, E. C., Agid, Y. & Graybiel, A. M. The substantia nigra of the human brain. II. Patterns of loss of dopamine-containing neurons in Parkinson's disease. *Brain* **122 (Pt 8**, 1437–48 (1999).
9. Mink, J. W. The basal ganglia: focused selection and inhibition of competing motor programs. *Prog. Neurobiol.* **50**, 381–425 (1996).
10. Albin, R. L., Young, A. B. & Penney, J. B. The functional anatomy of basal ganglia disorders. *Trends Neurosci.* **12**, 366–75 (1989).
11. DeLong, M. R. Primate models of movement disorders of basal ganglia origin. *Trends Neurosci.* **13**, 281–5 (1990).
12. Penney, J. B. & Young, A. B. Speculations on the functional anatomy of basal ganglia disorders. *Annu. Rev. Neurosci.* **6**, 73–94 (1983).
13. DeLong, M. R. & Wichmann, T. Circuits and circuit disorders of the basal ganglia. *Arch. Neurol.* **64**, 20–24 (2007).
14. Ahlskog, J. E. Beating a dead horse: dopamine and Parkinson disease. *Neurology* **69**, 1701–11 (2007).
15. Moore, D. J., West, A. B., Dawson, V. L. & Dawson, T. M. Molecular pathophysiology of Parkinson's disease. *Annu. Rev. Neurosci.* **28**, 57–87 (2005).
16. Burke, R. E., Dauer, W. T. & Vonsattel, J. P. G. A critical evaluation of the Braak staging scheme for Parkinson's disease. *Ann. Neurol.* **64**, 485–491 (2008).
17. Brooks, D. J. Examining Braak's hypothesis by imaging Parkinson's disease. *Mov. Disord.* **25 Suppl 1**, S83-8 (2010).
18. Goetz, C. G. *et al.* Movement Disorder Society Task Force report on the Hoehn and Yahr staging scale: status and recommendations. *Mov. Disord.* **19**, 1020–8 (2004).
19. Goetz, C. G. *et al.* Movement Disorder Society-sponsored revision of the Unified Parkinson's Disease Rating Scale (MDS-UPDRS): scale presentation and clinimetric testing results. *Mov. Disord.* **23**, 2129–70 (2008).
20. Hoehn, M. M. & Yahr, M. D. Parkinsonism: onset, progression, and mortality. *Neurology* **17**, 427–427 (1967).

21. Fahn, S., Marsden, C. D., Goldstein, M. & Calne, D. B. Recent Developments in Parkinson's Disease. in *Recent Developments in Parkinson's Disease* 153–163 (Macmillan Healthcare Information, 1987).
22. Cotzias, G. C., Papavasiliou, P. S. & Gellene, R. Modification of Parkinsonism — Chronic Treatment with L-Dopa. *N. Engl. J. Med.* **280**, 337–345 (1969).
23. Benabid, A. L., Pollak, P., Louveau, A., Henry, S. & de Rougemont, J. Combined (thalamotomy and stimulation) stereotactic surgery of the VIM thalamic nucleus for bilateral Parkinson disease. *Appl. Neurophysiol.* **50**, 344–6 (1987).
24. Jankovic, J. & Aguilar, L. G. Current approaches to the treatment of Parkinson's disease. *Neuropsychiatr. Dis. Treat.* **4**, 743–57 (2008).
25. Barbeau, A. L-dopa therapy in Parkinson's disease: a critical review of nine years' experience. *Can. Med. Assoc. J.* **101**, 59–68 (1969).
26. Cotzias, G. C. Levodopa in the Treatment of Parkinsonism. *JAMA J. Am. Med. Assoc.* **218**, 1903 (1971).
27. Schuurman, P. R. *et al.* A comparison of continuous thalamic stimulation and thalamotomy for suppression of severe tremor. *N. Engl. J. Med.* **342**, 461–8 (2000).
28. de Bie, R. M. A. *et al.* Morbidity and mortality following pallidotomy in Parkinson's disease: a systematic review. *Neurology* **58**, 1008–12 (2002).
29. Alvarez, L. *et al.* Bilateral subthalamotomy in Parkinson's disease: initial and long-term response. *Brain* **128**, 570–83 (2005).
30. Lai, E. C., Jankovic, J., Krauss, J. K., Ondo, W. G. & Grossman, R. G. Long-term efficacy of posteroventral pallidotomy in the treatment of Parkinson's disease. *Neurology* **55**, 1218–22 (2000).
31. Rodriguez-Oroz, M. C. *et al.* Bilateral deep brain stimulation in Parkinson's disease: a multicentre study with 4 years follow-up. *Brain* **128**, 2240–2249 (2005).
32. Deuschl, G. *et al.* A Randomized Trial of Deep-Brain Stimulation for Parkinson's Disease. *N. Engl. J. Med.* **355**, 896–908 (2006).
33. Moro, E. *et al.* Long-term results of a multicenter study on subthalamic and pallidal stimulation in Parkinson's disease. *Mov. Disord.* **25**, 578–586 (2010).
34. Group, T. D. B. S. for P. D. S. Deep-Brain Stimulation of the Subthalamic Nucleus or the Pars Interna of the Globus Pallidus in Parkinson's Disease. *N. Engl. J. Med.* **345**, 956–963 (2001).
35. Durif, F., Lemaire, J. J., Debilly, B. & Dordain, G. Long-term follow-up of globus pallidus chronic stimulation in advanced Parkinson's disease. *Mov. Disord.* **17**, 803–807 (2002).
36. Kleiner-Fisman, G. *et al.* Subthalamic nucleus deep brain stimulation: Summary and meta-analysis of outcomes. *Mov. Disord.* **21**, 290–304 (2006).
37. Okun, M. S. Deep-brain stimulation for Parkinson's disease. *N. Engl. J. Med.* **367**, 1529–38 (2012).
38. Minguez-Castellanos, A. *et al.* Different patterns of medication change after subthalamic or pallidal stimulation for Parkinson's disease: target related effect or selection bias? *J. Neurol. Neurosurg. Psychiatry* **76**, 34–9 (2005).
39. Anderson VC *et al.* Pallidal vs subthalamic nucleus deep brain stimulation in parkinson disease. *Arch. Neurol.* **62**, 554–560 (2005).
40. Follett, K. A. *et al.* Pallidal versus Subthalamic Deep-Brain Stimulation for Parkinson's Disease. *N. Engl. J. Med.* **362**, 2077–2091 (2010).

41. Odekerken, V. J. J. *et al.* Subthalamic nucleus versus globus pallidus bilateral deep brain stimulation for advanced Parkinson's disease (NSTAPS study): A randomised controlled trial. *Lancet Neurol.* **12**, 37–44 (2013).
42. Okun, M. S. & Foote, K. D. Subthalamic nucleus vs globus pallidus interna deep brain stimulation, the rematch: will pallidal deep brain stimulation make a triumphant return? *Arch. Neurol.* **62**, 533–6 (2005).
43. Benazzouz, A. *et al.* Effect of high-frequency stimulation of the subthalamic nucleus on the neuronal activities of the substantia nigra pars reticulata and ventrolateral nucleus of the thalamus in the rat. *Neuroscience* **99**, 289–95 (2000).
44. Dostrovsky, J. O. *et al.* Microstimulation-induced inhibition of neuronal firing in human globus pallidus. *J. Neurophysiol.* **84**, 570–4 (2000).
45. Hashimoto, T., Elder, C. M., Okun, M. S., Patrick, S. K. & Vitek, J. L. Stimulation of the subthalamic nucleus changes the firing pattern of pallidal neurons. *J. Neurosci.* **23**, 1916–23 (2003).
46. McIntyre, C. C., Grill, W. M., Sherman, D. L. & Thakor, N. V. Cellular effects of deep brain stimulation: model-based analysis of activation and inhibition. *J. Neurophysiol.* **91**, 1457–69 (2004).
47. Welter, M.-L. *et al.* Effects of high-frequency stimulation on subthalamic neuronal activity in parkinsonian patients. *Arch. Neurol.* **61**, 89–96 (2004).
48. Meissner, W. *et al.* Subthalamic high frequency stimulation resets subthalamic firing and reduces abnormal oscillations. *Brain* **128**, 2372–82 (2005).
49. Vitek, J. L., Zhang, J., Hashimoto, T., Russo, G. S. & Baker, K. B. External pallidal stimulation improves parkinsonian motor signs and modulates neuronal activity throughout the basal ganglia thalamic network. *Exp. Neurol.* **233**, 581–6 (2012).
50. Grill, W. M., Snyder, A. N. & Miocinovic, S. Deep brain stimulation creates an informational lesion of the stimulated nucleus. *Neuroreport* **15**, 1137–1140 (2004).
51. Dorval, A. D. *et al.* Deep Brain Stimulation Reduces Neuronal Entropy in the MPTP-Primate Model of Parkinson's Disease. *J. Neurophysiol.* **100**, 2807–2818 (2008).
52. Agnesi, F., Connolly, A. T., Baker, K. B., Vitek, J. L. & Johnson, M. D. Deep Brain Stimulation Imposes Complex Informational Lesions. *PLoS One* **8**, e74462 (2013).
53. Dorval, A. D., Kuncel, A. M., Birdno, M. J., Turner, D. A. & Grill, W. M. Deep Brain Stimulation Alleviates Parkinsonian Bradykinesia by Regularizing Pallidal Activity. *J. Neurophysiol.* **104**, 911–921 (2010).
54. Gilbertson, T. Existing Motor State Is Favored at the Expense of New Movement during 13-35 Hz Oscillatory Synchrony in the Human Corticospinal System. *J. Neurosci.* **25**, 7771–7779 (2005).
55. Brown, P. *et al.* Dopamine dependency of oscillations between subthalamic nucleus and pallidum in Parkinson's disease. *J. Neurosci.* **21**, 1033–8 (2001).
56. Levy, R. *et al.* Dependence of subthalamic nucleus oscillations on movement and dopamine in Parkinson's disease. *Brain* **125**, 1196–209 (2002).
57. Brown, P. Abnormal oscillatory synchronisation in the motor system leads to impaired movement. *Curr. Opin. Neurobiol.* **17**, 656–664 (2007).
58. Kühn, A. A., Kupsch, A., Schneider, G.-H. & Brown, P. Reduction in subthalamic 8-35 Hz oscillatory activity correlates with clinical improvement in Parkinson's disease. *Eur. J. Neurosci.* **23**, 1956–60 (2006).

59. Bronte-Stewart, H. *et al.* The STN beta-band profile in Parkinson's disease is stationary and shows prolonged attenuation after deep brain stimulation. *Exp. Neurol.* **215**, 20–28 (2009).
60. Eusebio, A. *et al.* Deep brain stimulation can suppress pathological synchronisation in parkinsonian patients. *J. Neurol. Neurosurg. Psychiatry* **82**, 569–573 (2011).
61. Wang, D. D. *et al.* Pallidal deep-brain stimulation disrupts pallidal beta oscillations and coherence with primary motor cortex in Parkinson's disease. *J. Neurosci.* **38**, 4556–4568 (2018).
62. Quinn, E. J. *et al.* Beta Oscillations in Freely Moving Parkinson ' s Subjects Are Attenuated During Deep Brain Stimulation. **30**, 1750–1758 (2015).
63. Little, S. & Brown, P. What brain signals are suitable for feedback control of deep brain stimulation in Parkinson's disease? *Ann. N. Y. Acad. Sci.* **1265**, 9–24 (2012).
64. Perera, T. *et al.* Deep brain stimulation wash-in and wash-out times for tremor and speech. *Brain Stimul.* **8**, 359 (2015).
65. Lopiano, L. *et al.* Temporal changes in movement time during the switch of the stimulators in Parkinson's disease patients treated by subthalamic nucleus stimulation. *Eur. Neurol.* **50**, 94–9 (2003).
66. Agnesi, F., Johnson, M. D. & Vitek, J. L. *Brain Stimulation: Chapter 4. Deep brain stimulation: how does it work?* (Elsevier Science, 2013).
67. Temperli, P. *et al.* How do parkinsonian signs return after discontinuation of subthalamic DBS? *Neurology* **60**, 78–81 (2003).
68. Cooper, S. E., Noecker, A. M., Abboud, H., Vitek, J. L. & McIntyre, C. C. Return of bradykinesia after subthalamic stimulation ceases: Relationship to electrode location. *Exp. Neurol.* **231**, 207–213 (2011).
69. Machado, A. *et al.* Deep brain stimulation for Parkinson's disease: surgical technique and perioperative management. *Mov. Disord.* **21 Suppl 1**, S247-58 (2006).
70. Miocinovic, S., Noecker, A. M., Maks, C. B., Butson, C. R. & McIntyre, C. C. Cicerone: stereotactic neurophysiological recording and deep brain stimulation electrode placement software system. *Acta Neurochir. Suppl.* **97**, 561–7 (2007).
71. Horn, A. & Kühn, A. A. Lead-DBS: a toolbox for deep brain stimulation electrode localizations and visualizations. *Neuroimage* **107**, 127–135 (2015).
72. Duchin, Y. *et al.* Patient-specific anatomical model for deep brain stimulation based on 7 Tesla MRI. *PLoS One* **13**, e0201469 (2018).
73. Husch, A., V Petersen, M., Gemmar, P., Goncalves, J. & Hertel, F. PaCER - A fully automated method for electrode trajectory and contact reconstruction in deep brain stimulation. *NeuroImage. Clin.* **17**, 80–89 (2018).
74. Horn, A. *et al.* Lead-DBS v2: Towards a comprehensive pipeline for deep brain stimulation imaging. *Neuroimage* **184**, 293–316 (2019).
75. Nickl, R. C. *et al.* Rescuing Suboptimal Outcomes of Subthalamic Deep Brain Stimulation in Parkinson Disease by Surgical Lead Revision. *Neurosurgery* **85**, E314–E321 (2019).
76. Volkmann, J., Moro, E. & Pahwa, R. Basic algorithms for the programming of deep brain stimulation in Parkinson's disease. *Mov. Disord.* **21**, 284–289 (2006).
77. Peña, E., Zhang, S., Deyo, S., Xiao, Y. & Johnson, M. D. Particle swarm optimization for programming deep brain stimulation arrays. *J. Neural Eng.* **14**,

016014 (2017).
78. Anderson, D. N., Osting, B., Vorwerk, J., Dorval, A. D. & Butson, C. R. Optimized programming algorithm for cylindrical and directional deep brain stimulation electrodes. *J. Neural Eng.* **15**, 026005 (2018).
79. Butson, C. R. & McIntyre, C. C. Current steering to control the volume of tissue activated during deep brain stimulation. *Brain Stimul.* **1**, 7–15 (2008).
80. Chaturvedi, A., Foutz, T. J. & McIntyre, C. C. Current steering to activate targeted neural pathways during deep brain stimulation of the subthalamic region. *Brain Stimul.* **5**, 369–377 (2012).
81. Barbe, M. T., Maarouf, M., Alesch, F. & Timmermann, L. Multiple source current steering – A novel deep brain stimulation concept for customized programming in a Parkinson's disease patient. *Parkinsonism Relat. Disord.* **20**, 471–473 (2014).
82. Limousin, P. *et al.* Abnormal involuntary movements induced by subthalamic nucleus stimulation in parkinsonian patients. *Mov. Disord.* **11**, 231–5 (1996).
83. Krack, P. *et al.* From off-period dystonia to peak-dose chorea. The clinical spectrum of varying subthalamic nucleus activity. *Brain* **122 (Pt 6**, 1133–46 (1999).
84. Zheng, Z. *et al.* Stimulation-induced dyskinesia in the early stage after subthalamic deep brain stimulation. *Stereotact. Funct. Neurosurg.* **88**, 29–34 (2010).
85. Wojtecki, L. *et al.* Frequency-Dependent Reciprocal Modulation of Verbal Fluency and Motor Functions in Subthalamic Deep Brain Stimulation. *Arch. Neurol.* **63**, 1273 (2006).
86. Okun, M. S. Mood changes with deep brain stimulation of STN and GPi: results of a pilot study. *J. Neurol. Neurosurg. Psychiatry* **74**, 1584–1586 (2003).
87. Merkl, A., Röck, E., Schmitz-Hübsch, T., Schneider, G. H. & Kühn, A. A. Effects of subthalamic nucleus deep brain stimulation on emotional working memory capacity and mood in patients with parkinson's disease. *Neuropsychiatr. Dis. Treat.* **13**, 1603–1611 (2017).
88. Volkmann, J. *et al.* Safety and efficacy of pallidal or subthalamic nucleus stimulation in advanced PD. *Neurology* **56**, 548–51 (2001).
89. Groiss, S. J., Wojtecki, L., Südmeyer, M. & Schnitzler, A. Deep brain stimulation in Parkinson's disease. *Ther. Adv. Neurol. Disord.* **2**, 20–8 (2009).
90. Little, S. *et al.* Adaptive deep brain stimulation in advanced Parkinson disease. *Ann. Neurol.* **74**, 449–57 (2013).
91. Little, S. *et al.* Bilateral adaptive deep brain stimulation is effective in Parkinson's disease. *J. Neurol. Neurosurg. Psychiatry* **87**, 717–721 (2016).
92. Little, S. *et al.* Adaptive deep brain stimulation for Parkinson's disease demonstrates reduced speech side effects compared to conventional stimulation in the acute setting. *Journal of Neurology, Neurosurgery and Psychiatry* (2016). doi:10.1136/jnnp-2016-313518
93. Velisar, A. *et al.* Dual threshold neural closed loop deep brain stimulation in Parkinson disease patients. *Brain Stimul.* **12**, 868–876 (2019).
94. Swann, N. C. *et al.* Adaptive deep brain stimulation for Parkinson's disease using motor cortex sensing. *J. Neural Eng.* **15**, 046006 (2018).
95. Herron, J. A. *et al.* Cortical Brain-Computer Interface for Closed-Loop Deep Brain Stimulation. *IEEE Trans. Neural Syst. Rehabil. Eng.* **25**, 2180–2187 (2017).
96. Cagnan, H. *et al.* Stimulating at the right time : phase-specific deep brain stimulation

Stimulating at the right time : phase-specific deep brain stimulation. *Brain* 132–145 (2016). doi:10.1093/aww308
97. Volkmann, J., Herzog, J., Kopper, F. & Geuschl, G. Introduction to the programming of deep brain stimulators. *Mov. Disord.* **17**, (2002).
98. Prochazka, A. *et al.* Measurement of Rigidity in Parkinson ' s Disease. *Mov. Disord.* **12**, 24–32 (1997).
99. Fung, V. S. C., Burne, J. A. & Morris, J. G. L. Objective quantification of resting and activated Parkinsonian rigidity: A comparison of angular impulse and work scores. *Mov. Disord.* **15**, 48–55 (2000).
100. Shapiro, M. B. *et al.* Effects of STN DBS on Rigidity in Parkinson's Disease. *IEEE Trans. Neural Syst. Rehabil. Eng.* **15**, 173–181 (2007).
101. Perera, T. *et al.* A Palm-Worn Device to Quantify Rigidity in Parkinson's Disease. *J. Neurosci. Methods* **317**, 113–120 (2019).
102. Homann, C. N. *et al.* The bradykinesia akinesia incoordination test (BRAIN TEST(C)), an objective and user-friendly means to evaluate patients with parkinsonism. *Mov. Disord.* **15**, 641–647 (2000).
103. Jobbágy, Á., Harcos, P., Karoly, R. & Fazekas, G. Analysis of finger-tapping movement. *J. Neurosci. Methods* **141**, 29–39 (2005).
104. Tavares, A. L. T. *et al.* Quantitative measurements of alternating finger tapping in Parkinson's disease correlate with UPDRS motor disability and reveal the improvement in fine motor control from medication and deep brain stimulation. *Mov. Disord.* **20**, 1286–1298 (2005).
105. Koop, M. M., Andrzejewski, A., Hill, B. C., Heit, G. & Bronte-Stewart, H. M. Improvement in a quantitative measure of bradykinesia after microelectrode recording in patients with Parkinson's disease during deep brain stimulation surgery. *Mov. Disord.* **21**, 673–678 (2006).
106. Papapetropoulos, S. *et al.* Objective Quantification of Neuromotor Symptoms in Parkinson's Disease: Implementation of a Portable, Computerized Measurement Tool. *Parkinsons. Dis.* **2010**, 1–6 (2010).
107. Kim, J. W. *et al.* Quantification of bradykinesia during clinical finger taps using a gyrosensor in patients with Parkinson's disease. *Med. Biol. Eng. Comput.* **49**, 365–371 (2011).
108. Pal, G. & Goetz, C. G. Assessing Bradykinesia in Parkinsonian Disorders. *Front. Neurol.* **4**, 1–5 (2013).
109. Dai, H., Zhang, P. & Lueth, T. Quantitative Assessment of Parkinsonian Tremor Based on an Inertial Measurement Unit. *Sensors* **15**, 25055–25071 (2015).
110. Blin, O., Ferrandez, A. M., Pailhous, J. & Serratrice, G. Dopa-sensitive and Dopa-resistant gait parameters in Parkinson's disease. *J. Neurol. Sci.* **103**, 51–54 (1991).
111. Morris, M. E., Matyas, T. A., Iansek, R. & Summers, J. J. Temporal Stability of Gait in Parkinson's Disease. *Phys. Ther.* **76**, 763–777 (1996).
112. Hausdorff, J. M., Cudkowicz, M. E., Firtion, R., Wei, J. Y. & Goldberger, A. L. Gait variability and basal ganglia disorders: Stride-to-stride variations of gait cycle timing in Parkinson's disease and Huntington's disease. *Mov. Disord.* **13**, 428–437 (1998).
113. Schaafsma, J. D. *et al.* Gait dynamics in Parkinson's disease: relationship to Parkinsonian features, falls and response to levodopa. *J. Neurol. Sci.* **212**, 47–53

(2003).
114. Plotnik, M., Giladi, N. & Hausdorff, J. M. A new measure for quantifying the bilateral coordination of human gait: Effects of aging and Parkinson's disease. *Exp. Brain Res.* **181**, 561–570 (2007).
115. Pulliam, C. L. *et al.* Motion sensor strategies for automated optimization of deep brain stimulation in Parkinson's disease. *Parkinsonism Relat. Disord.* **21**, 378–382 (2015).
116. Heldman, D. A. *et al.* Computer-Guided Deep Brain Stimulation Programming for Parkinson's Disease. *Neuromodulation* **19**, 127–131 (2016).
117. Rizzone, M. Deep brain stimulation of the subthalamic nucleus in Parkinson's disease: effects of variation in stimulation parameters. *J. Neurol. Neurosurg. Psychiatry* **71**, 215–219 (2001).
118. Moro, E. *et al.* The impact on Parkinson's disease of electrical parameter settings in STN stimulation. *Neurology* **59**, 706–713 (2002).
119. Picillo, M., Lozano, A. M., Kou, N., Puppi Munhoz, R. & Fasano, A. Programming Deep Brain Stimulation for Parkinson's Disease: The Toronto Western Hospital Algorithms. *Brain Stimul.* (2016). doi:10.1016/j.brs.2016.02.004
120. Hamel, W. *et al.* Targeting of the Subthalamic Nucleus for Deep Brain Stimulation: A Survey Among Parkinson Disease Specialists. *World Neurosurg.* **99**, 41–46 (2017).
121. Butson, C. R., Cooper, S. E., Henderson, J. M., Wolgamuth, B. & McIntyre, C. C. Probabilistic analysis of activation volumes generated during deep brain stimulation. *Neuroimage* **54**, 2096–2104 (2011).
122. Hilliard, J. D., Frysinger, R. C. & Elias, W. J. Effective Subthalamic Nucleus Deep Brain Stimulation Sites May Differ for Tremor, Bradykinesia and Gait Disturbances in Parkinson's Disease. *Stereotact. Funct. Neurosurg.* **89**, 357–364 (2011).
123. Eisenstein, S. A. *et al.* Functional anatomy of subthalamic nucleus stimulation in Parkinson disease. *Ann. Neurol.* **76**, 279–295 (2014).
124. Linn-Evans, M. E. *et al.* REM sleep without atonia is associated with increased rigidity in patients with mild to moderate Parkinson's disease. *Clin. Neurophysiol.* (2020). doi:10.1016/j.clinph.2020.04.017
125. Limousin, P. *et al.* Effect of parkinsonian signs and symptoms of bilateral subthalamic nucleus stimulation. *Lancet (London, England)* **345**, 91–5 (1995).
126. Schrag, A., Jahanshahi, M. & Quinn, N. What contributes to quality of life in patients with Parkinson's disease? *J. Neurol. Neurosurg. Psychiatry* **69**, 308–312 (2000).
127. Mockus, J. Application of Bayesian approach to numerical methods of global and stochastic optimization. *J. Glob. Optim.* **4**, 347–365 (1994).
128. Jones, D. R., Schonlau, M. & Welch, W. J. Efficient Global Optimization of Expensive Black-Box Functions. *J. Glob. Optim.* **13**, 455–492 (1998).
129. Streltsov, S. & Vakili, P. A Non-myopic Utility Function for Statistical Global Optimization Algorithms. *J. Glob. Optim.* **14**, 283–298 (1999).
130. Jones, D. R. A Taxonomy of Global Optimization Methods Based on Response Surfaces. *J. Glob. Optim.* **21**, 345–383 (2001).
131. Brochu, E., Cora, V. M. & de Freitas, N. A Tutorial on Bayesian Optimization of Expensive Cost Functions, with Application to Active User Modeling and

Hierarchical Reinforcement Learning. (2010).
132. Rasmussen, C. E. & Williams, C. K. I. *Gaussian Processes for Machine Learning (Adaptive Computation and Machine Learning)*. (The MIT Press, 2005).
133. Matérn, B. *Spatial Variation*. **36**, (Springer New York, 1986).
134. Stein, M. L. *Interpolation of Spatial Data*. (Springer New York, 1999). doi:10.1007/978-1-4612-1494-6
135. Siegel, S. & Castellan Jr., N. J. *Nonparametric statistics for the behavioral sciences, 2nd ed. Nonparametric statistics for the behavioral sciences, 2nd ed.* (Mcgraw-Hill Book Company, 1988).
136. Payne, J. W., Bettman, J. R. & Johnson, E. J. *The Adaptive Decision Maker*. (Cambridge University Press, 1993). doi:10.1017/CBO9781139173933
137. Kingsley, D. C. & Brown, T. C. Preference Uncertainty, Preference Learning, and Paired Comparison Experiments. *Land Econ.* **86**, 530–544 (2010).
138. Kahneman, D. & Tversky, A. Prospect Theory: An Analysis of Decision under Risk. *Econometrica* **47**, 263 (1979).
139. Tversky, A. & Kahneman, D. Advances in prospect theory: Cumulative representation of uncertainty. *J. Risk Uncertain.* **5**, 297–323 (1992).
140. Khoo, H. M. *et al.* Low-frequency subthalamic nucleus stimulation in Parkinson's disease: A randomized clinical trial. *Mov. Disord.* **29**, 270–274 (2014).
141. Stegemöller, E. L. *et al.* Selective use of low frequency stimulation in Parkinson's disease based on absence of tremor. *NeuroRehabilitation* **33**, 305–312 (2013).
142. Okun, M. S. *et al.* Cognition and Mood in Parkinson Disease in STN versus GPi DBS: The COMPARE Trial. *Ann. Neurol.* **65**, 586–595 (2010).
143. Ramirez-Zamora, A. & Ostrem, J. L. Globus pallidus interna or subthalamic nucleus deep brain stimulation for Parkinson disease a review. *JAMA Neurol.* **75**, 367–372 (2018).
144. Holden, S. K., Finseth, T., Sillau, S. H. & Berman, B. D. Progression of MDS-UPDRS Scores Over Five Years in De Novo Parkinson Disease from the Parkinson's Progression Markers Initiative Cohort. *Mov. Disord. Clin. Pract.* **5**, 47–53 (2018).
145. Fasano, A. & Lozano, A. M. The FM/AM world is shaping the future of deep brain stimulation. *Mov. Disord.* **29**, 161–163 (2014).
146. Montgomery, E. & He, H. The FM/AM world is shaping the future of deep brain stimulation. *Mov. Disord.* **29**, 1327–1327 (2014).
147. Galna, B., Lord, S. & Rochester, L. Is gait variability reliable in older adults and Parkinson's disease? Towards an optimal testing protocol. *Gait Posture* **37**, 580–585 (2013).
148. Stolze, H. *et al.* Effects of bilateral subthalamic nucleus stimulation on parkinsonian gait. *Neurology* **57**, 144–6 (2001).
149. Faist, M. *et al.* Effect of bilateral subthalamic nucleus stimulation on gait in Parkinson's disease. *Brain* **124**, 1590–600 (2001).
150. Allert, N. *et al.* Effects of bilateral pallidal or subthalamic stimulation on gait in advanced Parkinson's disease. *Mov. Disord.* **16**, 1076–1085 (2001).
151. Xie, J., Krack, P., Benabid, A. L. & Pollak, P. Effect of bilateral subthalamic nucleus stimulation on parkinsonian gait. *J. Neurol.* **248**, 1068–1072 (2001).
152. Ferrarin, M. *et al.* Quantitative analysis of gait in Parkinson's disease: A pilot study

on the effects of bilateral sub-thalamic stimulation. *Gait Posture* **16**, 135–148 (2002).
153. Krystkowiak, P. *et al.* Effects of Subthalamic Nucleus Stimulation and Levodopa Treatment on Gait Abnormalities in Parkinson Disease. *Arch. Neurol.* **60**, 80–4 (2003).
154. Ferrarin, M. *et al.* Effects of bilateral subthalamic stimulation on gait kinematics and kinetics in Parkinson's disease. *Exp. Brain Res.* **160**, 517–527 (2005).
155. Piper, M., Abrams, G. M. & Marks, W. J. J. Deep brain stimulation for the treatment of Parkinson's disease: overview and impact on gait and mobility. *NeuroRehabilitation* **20**, 223–232 (2005).
156. Lubik, S. *et al.* Gait analysis in patients with advanced Parkinson disease: Different or additive effects on gait induced by levodopa and chronic STN stimulation. *J. Neural Transm.* **113**, 163–173 (2006).
157. Cantiniaux, S. *et al.* Comparative analysis of gait and speech in Parkinson's disease: Hypokinetic or dysrhythmic disorders? *J. Neurol. Neurosurg. Psychiatry* **81**, 177–184 (2010).
158. Fasano, A., Aquino, C. C., Krauss, J. K., Honey, C. R. & Bloem, B. R. Axial disability and deep brain stimulation in patients with Parkinson disease. *Nat. Rev. Neurol.* **11**, 98–110 (2015).
159. Munro-Davies, L. E., Winter, J., Aziz, T. Z. & Stein, J. F. The role of the pedunculopontine region in basal-ganglia mechanisms of akinesia. *Exp. Brain Res.* **129**, 0511–0517 (1999).
160. Pahapill, P. A. & Lozano, A. M. The pedunculopontine nucleus and Parkinson's disease. *Brain* **123 (Pt 9**, 1767–83 (2000).
161. Nandi, D., Aziz, T. Z., Giladi, N., Winter, J. & Stein, J. F. Reversal of akinesia in experimental parkinsonism by GABA antagonist microinjections in the pedunculopontine nucleus. *Brain* **125**, 2418–30 (2002).
162. Takakusaki, K., Habaguchi, T., Ohtinata-Sugimoto, J., Saitoh, K. & Sakamoto, T. Basal ganglia efferents to the brainstem centers controlling postural muscle tone and locomotion: a new concept for understanding motor disorders in basal ganglia dysfunction. *Neuroscience* **119**, 293–308 (2003).
163. Jenkinson, N. *et al.* Anatomy, physiology, and pathophysiology of the pedunculopontine nucleus. *Mov. Disord.* **24**, 319–328 (2009).
164. Morita, H. *et al.* Pedunculopontine nucleus stimulation: Where are we now and what needs to be done to move the field forward? *Front. Neurol.* **5**, (2014).
165. Little, S. *et al.* Controlling Parkinson's Disease With Adaptive Deep Brain Stimulation. *J. Vis. Exp.* (2014). doi:10.3791/51403
166. Rosa, M. *et al.* Adaptive deep brain stimulation in a freely moving parkinsonian patient. *Mov. Disord.* **30**, 1003–1005 (2015).
167. Singh, A. *et al.* Pattern of local field potential activity in the globus pallidus internum of dystonic patients during walking on a treadmill. *Exp. Neurol.* **232**, 162–167 (2011).
168. Hell, F., Plate, A., Mehrkens, J. H. & Bötzel, K. Subthalamic oscillatory activity and connectivity during gait in Parkinson's disease. *NeuroImage Clin.* **19**, 396–405 (2018).
169. Fischer, P. *et al.* Alternating Modulation of Subthalamic Nucleus Beta Oscillations

during Stepping. *J. Neurosci.* **38**, 5111–5121 (2018).
170. Kühn, A. A. *et al.* High-frequency stimulation of the subthalamic nucleus suppresses oscillatory β activity in patients with Parkinson's disease in parallel with improvement in motor performance. *J. Neurosci.* **28**, 6165–6173 (2008).
171. Wingeier, B. *et al.* Intra-operative STN DBS attenuates the prominent beta rhythm in the STN in Parkinson's disease. *Exp. Neurol.* **197**, 244–251 (2006).
172. Zhu, H. S., Wertsch, J. J., Harris, G. F., Loftsgaarden, J. D. & Price, M. B. Foot pressure distribution during walking and shuffling. *Arch. Phys. Med. Rehabil.* **72**, 390–7 (1991).
173. Iansek, R., Huxham, F. & McGinley, J. The sequence effect and gait festination in Parkinson disease: Contributors to freezing of gait? *Mov. Disord.* **21**, 1419–1424 (2006).
174. Chee, R., Murphy, A., Danoudis, M., Georgiou-Karistianis, N. & Iansek, R. Gait freezing in Parkinson's disease and the stride length sequence effect interaction. *Brain* **132**, 2151–2160 (2009).
175. Nieuwboer, A. & Giladi, N. Characterizing freezing of gait in Parkinson's disease: Models of an episodic phenomenon. *Mov. Disord.* **28**, 1509–1519 (2013).
176. Kirtley, C. Clinical gait analysis: theory and practice. xii, 316 p. (2006).
177. Bastian, A. J., Kelly, V. E., Revilla, F. J., Perlmutter, J. S. & Mink, J. W. Different Effects of Unilateral Versus Bilateral Subthalamic Nucleus Stimulation on Walking and Reaching in Parkinson ' s Disease. **18**, 1000–1007 (2003).
178. Johnsen, E. L., Mogensen, P. H., Sunde, N. A. & Østergaard, K. Improved asymmetry of gait in Parkinson's disease with DBS: gait and postural instability in Parkinson's disease treated with bilateral deep brain stimulation in the subthalamic nucleus. *Mov. Disord.* **24**, 590–7 (2009).
179. Johnsen, E. L., Sunde, N., Mogensen, P. H. & Østergaard, K. MRI verified STN stimulation site - Gait improvement and clinical outcome. *Eur. J. Neurol.* **17**, 746–753 (2010).
180. McNeely, M. E. *et al.* Effects of deep brain stimulation of dorsal versus ventral subthalamic nucleus regions on gait and balance in Parkinson's disease. *J. Neurol. Neurosurg. Psychiatry* **82**, 1250–1255 (2011).
181. Benarroch, E. E. Subthalamic nucleus and its connections: Anatomic substrate for the network effects of deep brain stimulation. *Neurology* **70**, 1991–1995 (2008).
182. Weaver, F. M. *et al.* Randomized trial of deep brain stimulation for Parkinson disease: thirty-six-month outcomes. *Neurology* **79**, 55–65 (2012).
183. Weaver, F. M. *et al.* Bilateral deep brain stimulation vs best medical therapy for patients with advanced Parkinson disease: a randomized controlled trial. *JAMA* **301**, 63–73 (2009).
184. Liu, W. *et al.* Bilateral subthalamic stimulation improves gait initiation in patients with Parkinson's disease. *Gait Posture* **23**, 492–498 (2006).
185. Powell, D., Hanson, N., Threlkeld, A. J., Fang, X. & Xia, R. Enhancement of parkinsonian rigidity with contralateral hand activation. *Clin. Neurophysiol.* **122**, 1595–601 (2011).
186. Stolze, H. *et al.* Prevalence of gait disorders in hospitalized neurological patients. *Mov. Disord.* **20**, 89–94 (2005).
187. Wood, B. H., Bilclough, J. A., Bowron, A. & Walker, R. W. Incidence and

prediction of falls in Parkinson's disease: a prospective multidisciplinary study. *J. Neurol. Neurosurg. Psychiatry* **72**, 721–5 (2002).
188. Sterling, M., Jull, G. & Wright, A. The effect of musculoskeletal pain on motor activity and control. *J. Pain* **2**, 135–145 (2001).